



OSLO METROPOLITAN UNIVERSITY
STORBYUNIVERSITETET

Department of Civil Engineering and Energy Technology
Energy and Environment in buildings

Mailing address: PB 4 St. Olavs plass, 0130 Oslo
Street address: Pilestredet 35, Oslo

GROUP/CANDIDATE NR.

401

AVAILABILITY

Open

Phone 67 23 50 00

www.oslomet.no

MASTER'S THESIS

TITLE	DATE
Energy performance and fire resistance of novel PCM	2022-01-01
	NUMBER OF PAGES /ATTACHMENTS
	50/3
AUTHOR	SUPERVISOR
Sebastian Bergesen	Arnab Chaudhuri Habtamu Bayera Madessa

DONE IN COLLABORATION WITH	CONTACT
Gyproc Saint-Gobain, Sweden AB	

ABSTRACT
<p>Cooling is the fastest-growing energy demand in buildings, with the prediction of energy for space cooling to triple by the year 2050. One of the interesting ways to tackle this problem is to reduce the energy load during cooling seasons by incorporating PCM. A problem that has kept occurring regarding PCM materials is their low resistance to fire. As such, Gyproc Saint-Gobain, Sweden AB is in the development of a novel PCM in the form of a spackle compound infused with fire retardants. Energy simulations were performed on an office building during summer climate in Oslo, Norway, with the novel PCM applied to interior walls and ceilings. The findings showed positive results regarding both thermal comfort and cooling load. It was evident that the impact of PCM was greatly influenced by other measures in the building, such as night ventilation and solar shading. Reducing the heat gain in the zone using effective solar shading had a substantial increase in the attractiveness of PCM, amplifying its impact on the building's energy efficiency. The materials fire performance, unfortunately, showed unsatisfactory results, and further improvement is required to fulfill necessary fire codes and standards.</p>

3 KEYWORDS
Novel PCM
Energy performance
Fire resistance

Summary

According to United Nations Environment Programme (2021): "Global Status Report for Buildings and Construction", the building sector accounted for 36% of the total energy demand, as well as 37% of energy-related CO_2 emissions in 2020 [1].

International Energy Agency (IEA) report that air conditioners and electric fans used for building cooling account for nearly 20% of the total energy use in buildings. Additionally, cooling is the fastest-growing energy demand in buildings, with the prediction of energy demand for space cooling to triple by the year 2050 [2].

Gyproc Saint-Gobain, Sweden AB is developing a novel construction material in which a spackle compound made up of various binding materials and paraffin-based micro-encapsulated phase-changing materials (PCM). Since the material absorbs and releases heat at very small or negligible temperature changes, it is ideal for latent heat storage. A new addition to this novel PCM is the introduction of fire retardants.

Multiple tests and simulations was conducted to analyze the properties of the novel PCM. A practical experiment was conducted in a climate chamber situated on OsloMet. By measuring the heat flux through the material using the TRSYS01 heat flux measuring system, thermal conductivity of the material was determined to have a value of $k \approx 0.093 \frac{W}{m^2K}$. Energy simulations were performed on a validated TEK-17 building in Oslo, Norway, during the summertime, with multiple variations of PCM, night ventilation, and shading devices. Several aspects, including peak load shift, peak temperature, and indoor temperature change, were investigated to assess the influence of the novel PCM. A cone calorimeter test was performed on Lund university to collect information regarding fire performance.

Energy simulations showed that PCM worked as intended under the right conditions, reducing the local cooling load by an additional 28%. PCM also effected the diurnal thermal fluctuations, as well as kept the cubicles at a desired thermal comfort level for a longer period. The benefits from better solar shading was also evident, increasing the effectiveness of PCM. Higher amounts of PCM showed to be more beneficial when the thermal gain in the cubicle were high, but became an unnecessary measure when the building had reduced solar gain. Better control over heat gains in the zones was found to be an important variable when introducing PCM to the building mass. The fire performance of the material showed unsatisfactory results, and improvements to fire retardation is required to fulfill necessary fire codes and standards.

A sensitivity analysis on the energy performance of the novel PCM spackle were performed varying the thermal conductivity in the range [0.08 to 0.11 W/m.K]. The results revealed negligible variations in the energy efficiency simulations.

Sammendrag

I følge FNs miljøprogram (2021): "Global Status Report for Buildings and Construction" sto byggesektoren for 36% av det totale energibehovet, samt 37% av energirelaterte CO_2 -utslipp i 2020 [1].

Det internasjonale energibyrået (IEA) rapporterer at klimaanlegg og elektriske vifter som brukes til kjøling av bygninger står for nesten 20% av den totale energibruken i bygninger. I tillegg er kjøling det raskest voksende energibehovet i bygninger, med prosjekteringer at energibehovet for romkjøling vil tredobles innen år 2050 [2].

Gyproc Saint-Gobain, Sverige AB holder på med utvikling av et nytt konstruksjonsmateriale der en sparkel-blanding bestående av ulike bindematerialer og parafinbaserte mikroinnkapslede faseendrende materialer (PCM). Siden materialet absorberer og avgir varme ved svært små eller ubetydelige temperaturendringer, er det ideelt for latent varmelagring i bygninger. Et nytt tillegg til denne nye PCM'en er introduksjonen av brannhemmende midler.

Flere tester og simuleringer ble utført for å analysere egenskapene til dette nye materialet. Et praktisk eksperiment ble utført i et klimakammer på OsloMet. Ved å måle varmekraften gjennom materialet ved å bruke TRSYS01 varmekraft målesystemet, ble varmeledningsevnen til materialet bestemt til å ha en verdi på $k \approx 0.093 \frac{W}{m^2K}$. Energisimuleringer ble utført på en validert TEK-17-bygning i Oslo, Norge, om sommeren, med flere varianter av PCM, nattventilasjon og solskjerming. Flere aspekter, inkludert elektrisk topplastforskyvning, maks operativ temperatur og innendørstemperaturendring, ble undersøkt for å vurdere påvirkningen av den nye materialet. En "cone calorimeter test" ble utført på Lund university der brannytelse ble undersøkt.

Energisimuleringer viste at PCM fungerte etter hensikten under de rette forholdene, og reduserte den lokale kjølebelastningen med 28%. PCM påvirket også de daglige termiske svingningene, samt forlenget ønsket termisk komfortnivå. Fordelene med bedre solskjerming var også tydelig, og førte til økt effektiviteten av PCM. Høyere mengder PCM viste seg å være mer fordelaktig når den termiske gevinsten i sonen var høy, men hviste seg å være et unødvendig tiltak når bygget hadde redusert solenergi. Bedre kontroll over varmegevinster i sonene ble funnet å være en viktig variabel ved introduksjon av PCM til bygningsmassen. Brannytelsen til materialet viste utifredstillende resultater, og forbedringer av brannhemming er nødvendig for å oppfylle nødvendige brannforskrifter og standarder.

En sensitivitetsanalyse på energiytelsen til den nye PCM-sparkellet ble utført med varierende varmeledningsevne i området $[0,08 \text{ til } 0,11 \text{ W/m}]$. Resultatene avdekket ubetydelige variasjoner i energieffektivitetssimuleringene.

Preface

This master thesis was written in spring 2022 at the Department of Civil Engineering and Energy Technology at Oslo Metropolitan University. And was made possible with the help from Gyproc.

I would first like to thank my supervisors Arnab Chaudhuri and Habtamu Bayera Madessa for all the time and energy you put in to help me write this thesis.

I would also like to thank Andreas Aamodt for taking the time to help me with my numerical simulations, but also as a great supporter during the whole process. The valuable assistance from Nils Ledermann during my practical experiments must also be mentioned, providing me with helpful input and interest.

Last but not least, a great appreciation goes out to my wonderful classmates who have made these 5 years on Oslomet extremely enjoyable.


Sebastian Bergesen

Oslo, 25.05.2022

Contents

1	Introduction	1
1.1	Background	1
1.2	Phase change materials for energy efficiency	2
1.3	Fire resistance properties of PCM materials	3
1.4	Formulation of the research question	3
2	Theory	4
2.1	Thermal heat storage	4
3	Methodology	6
3.1	Climate room experiment	6
3.2	Instrument principle and theory	11
3.3	Determining thermal conductivity	15
3.3.1	Material properties	15
3.3.2	Fire performance	16
3.4	Energy simulation	17
3.5	Description of the building	18
3.5.1	Office cubicles	18
3.5.2	Climate	20
3.6	PCM energy performance	21
3.6.1	Increasing PCM effectiveness using night ventilation	21
3.6.2	Solar shading	23
3.6.3	Simulation cases	24
3.6.4	Energy efficiency calculations	25
3.6.5	Solidification of the PCM	25
4	Results and discussion	27
4.1	Steady-state experiment	27
4.2	Numerical simulations	29
4.2.1	Effect of different parameters	29
4.2.2	Energy analysis	36
4.2.3	Solidification of PCM	44
4.2.4	Fire performance	45
4.2.5	Uncertainties and sensitivity analysis	46
5	Conclusion	48
5.1	Future work	49

A PCM properties	54
B Input data report	55
C Shading properties	57
D Measurements from the Hukseflux TRSYS01 system	59

1. Introduction

1.1 Background

It is well-known that the building sector accounts for a large portion of the total energy consumption on a global scale. According to United Nations Environment Programme (2021): "Global Status Report for Buildings and Construction", the building sector accounted for 36% of the total energy demand, as well as 37% of energy-related CO_2 emissions in 2020 [1]. It is also possible that these values will rise over time as global living standards improve. Today, finite fossil fuel supplies and concerns about greenhouse gas emissions make efficient energy use a critical issue.

As a result, multiple policies such as the "Paris agreement" and "European green deal" have been implemented to reduce these numbers worldwide [3]. European Union (EU) policies emphasize energy efficiency and renewable production in order to achieve climate neutrality by 2050. This ambitious target, as stated in the European Green Deal, necessitates maximizing energy efficiency and renewable production in industry, mobility, economy, and agriculture [4][5]. Research focusing on reducing the energy consumption in buildings can also be seen as a vital part of the quest to steer the world to a more sustainable and safe future.

The national standards for buildings are therefore constantly evolving in many regions of the world, including Norway. With the introduction of new standards, the building body has come a long way in its ability to reduce thermal loss. This however poses a problem with high temperatures during the cooling season.

This especially holds true when considering the current change in the global climate. According to the International Energy Agency (IEA), air conditioners and electric fans used for building cooling account for nearly 20% of the total energy use in buildings. Additionally, cooling is the fastest-growing energy demand in buildings, with the prediction of energy demand for space cooling to triple by the year 2050 [2]. For these reasons, the relevance of cooling techniques will continue to increase in the near future [6]. As the building body needs to limit the increase of internal temperature during the day, solutions that circumvent the need to use extra energy would be beneficial. Therefore, the more sought-after techniques are passive cooling solutions, which is the basis of this thesis.

Earlier studies have already proven that passive cooling such as night ventilation (NV) can be a significant and important tool to further reduce thermal discomfort and energy demand during cooling seasons[7] [8]. Gyproc Saint-Gobain, Sweden AB is developing a novel construction material in which a spackle compound is made up of various binding materials and paraffin-based micro-encapsulated phase-changing materials (PCM). With the purpose of greatly increasing the thermal inertia of a building when applied to interior constructions. Paraffin-based PCM is highly suitable in buildings as the melting temperature is around the human comfort level.

The purpose of this study is to evaluate the novel PCM in real-life conditions, by doing practical experiments to gain information about the properties of the material, and using the acquired

data to perform numerical simulations on an office building modeled after TEK-17. Results gathered from the simulations will then be analyzed in hopes to better understand its effect on the building's energy efficiency. Properties related to fire resistance and Euroclass will also be investigated.

1.2 Phase change materials for energy efficiency

For the reasons mentioned above, there has been a higher interest in ways to lower the cooling load of buildings. One of the promising methods that have emerged in literature over the years is the application of PCM, with its advantageous properties connected to thermal storage.

Thermal energy storage (TES), namely sensible heat storage (SHS) has already been used in the building industry for a long time but requires heavyweight constructions with high density. The concept is based on the change in heat capacity and temperature of the material during the charging and discharging process. Utilizing this correctly can give positive impacts on a building, such as delaying the peak load, increasing thermal inertia, as well as reducing heating and cooling loads. The major difference between the conventional TES materials and PCM is the usage of latent heat storage (LHS). LHS is one of the more efficient applications of THS, and is based on the concept of storing and releasing thermal energy as the material undergoes a change in phase, for example, solid to liquid, liquid to gas, and vice versa. As such, the conventional materials used for heat storage such as concrete require a much bigger volume to achieve the same results as PCM, as the effectiveness of materials using SHS is much lower than LHS[9].

Unlike conventional sensible storage materials, when PCM reaches the temperature at which it changes phase, they absorb a large amount of heat without getting hotter. As the temperature drops and the PCM starts to solidify, the stored latent heat gets released[10].

Since the material absorbs and releases heat at very small or negligible temperature changes, it is ideal for latent heat storage. The incorporation of phase change materials into buildings has already been shown to be a promising alternative for increasing a building's thermal storage capacity, and as a result, lowering cooling loads [11].

Furthermore, practical PCM benefits from having upper and lower phase transition temperatures that are within the application's operational temperature range, as well as high thermal conductivity for effective heat transmission. The melting point of PCM is crucial when used for free cooling. And should be chosen in such a way that it ensures maximum solidification during the charging process, while also keeping the ambient temperature within acceptable limits during the day. [12]

For this reason, paraffin-based PCM is highly suitable in buildings as the melting temperature is around the human comfort level. In this thesis, the spackle infused with the novel paraffin-based PCM will be applied to the interior gypsum boards. This will provide increased thermal storage distributed through the building, hopefully resulting in off-peak hour cooling loads, as well as favorable temperature developments.

Because this thesis is somewhat a continuation of the work by Aamodt et al., a full literature review is not included to reduce redundancy. A short summary of the review findings will instead be included: Thermal comfort and energy savings potential with PCMs have already been examined in several experimental and numerical investigations. The outcomes are generally positive, although they vary throughout each case. This is not surprising, given the multitude of variables that influence the material's efficiency. PCMs are also developed in a variety of configurations, with various approaches regarding implementation. The results are clearly dependent on the PCM used in the study, the experimental design parameters employed, and the numerical model input data.

1.3 Fire resistance properties of PCM materials

One problem that has continued to halt the advances of PCM-infused materials is their low resistance to fire. This is also one of the main concerns when using paraffin-based PCM, as it can catch fire if not properly protected [13] [14]. According to TEK-17, a building material that is meant to be used on interior walls and ceilings requires at least a Euroclass of B or higher. Which for the reason mentioned has often been shown to be problematic. The biggest change in the material compared to the one investigated by Aamodt et al. is the new incorporation of fire retardants. This new addition to the material will hopefully increase its fire performance, without compromising its energy efficiency. To get a better understanding of the material at hand, a cone calorimeter test was performed at Lund University, and the data obtained will be used by the simulation program Conetools.

1.4 Formulation of the research question

To start the thesis, some research questions must be set. As this novel PCM has not been properly investigated before, multiple aspects regarding the material will be under review.

1. What is the heat conductivity of the material at hand?
2. What changes occur to the operative temperature when the material is applied to an up-to-code building under Norwegian summer conditions, and what consequences does this pose to the cooling load?
3. What building conditions are optimal for the novel PCM to be fully utilized?
4. Is the fire performance of the material good enough to be used in a real-life application?

2. Theory

2.1 Thermal heat storage

Thermal heat storage is the intermediate storage of thermal energy by either heating or cooling a storage material so that the stored energy in the material can be used at a later time for either heating or cooling. Thermal energy can be stored as a change in a material's internal energy as sensible heat, latent heat, thermochemical, or a combination of these.[15]

Sensible heat storage

Thermal energy is stored in sensible heat storage (SHS) by increasing the temperature of a solid or liquid. The heat capacity and temperature change of the material during the charging and discharging processes are used by the SHS system. The amount of heat stored is determined by the specific heat of the medium, the temperature change, and the amount of storage material used.

Latent heat storage with PCM

Latent heat storage (LHS) is a very attractive technique, as it provides a high energy storage density and the ability to store heat as latent heat of fusion at a constant temperature corresponding to the phase transition temperature of phase change materials [16]. When a material transitions from solid to liquid, it absorbs energy from its environment while maintaining a constant or almost constant temperature. The absorbed energy acts to increase the energy of the constituent atoms or molecules, thus increasing their vibrational state. The atomic bonds loosen as the substance transforms from a solid to a liquid at the melt temperature. Solidification is the inverse of this process, in which the material sends energy to its surroundings while the molecules lose energy and arrange themselves into their solid phase[17]. Figure 2.1 from Amy S. Fleischer's book shows how a material's thermal storage changes in regards to temperature and energy addition.

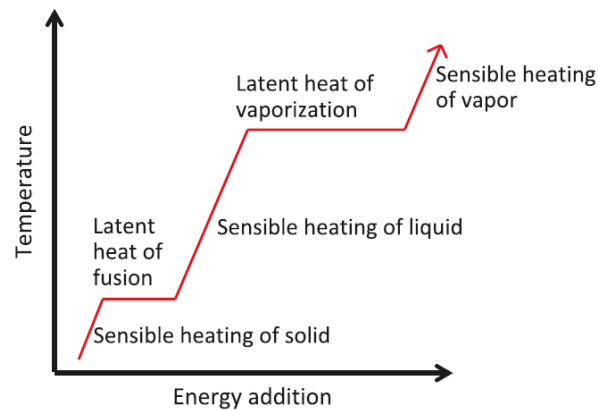


Figure 2.1: Standard heating curve

PCM and micro encapsulation

Today, the benefits of thermal heat storage in the envelope can be gained by utilizing advanced building products that employ new smart materials such as phase-change materials, capable of accumulating and releasing external heat via the phase transition phenomenon while maintaining a steady internal temperature. For PCMs in buildings to perform to the best of their ability, the temperature must exceed the melting point during the day and allow a phase transition, then drop below the melting point to start a new cycle the following day. The majority of the energy stored in a full daily cycle originates from latent heat absorbed by the PCM volume while the PCM is melting; after that, only sensible heat is absorbed, with a much lower thermal capacity.[18] It is therefore important to choose a PCM with an operational range in between the temperature variations of its environment.

One of the ways to incorporate PCM to materials is through the use of micro-encapsulation. The scale of the typical micro-encapsulated PCM is 1–1000 μm in diameter and uses polymeric shells which encapsulate the PCM core. There are multiple ways to create encapsulated PCM both with physical methods and with the more common chemical method. Because phase separation is constrained to microscopic distances, micro-encapsulation also helps to improve the stability of the fusion solidification cycle.

3. Methodology

In order to extract information about the PCM spackle, both experimental studies and numerical approaches were used. Multiple tests and simulations were conducted to analyze the properties of the novel PCM. Many aspects were explored to determine the impact of the novel PCM in an office building, including peak load shifting, peak temperature, and indoor temperature variation. A flowchart of the methodology of the thesis is shown in 3.1

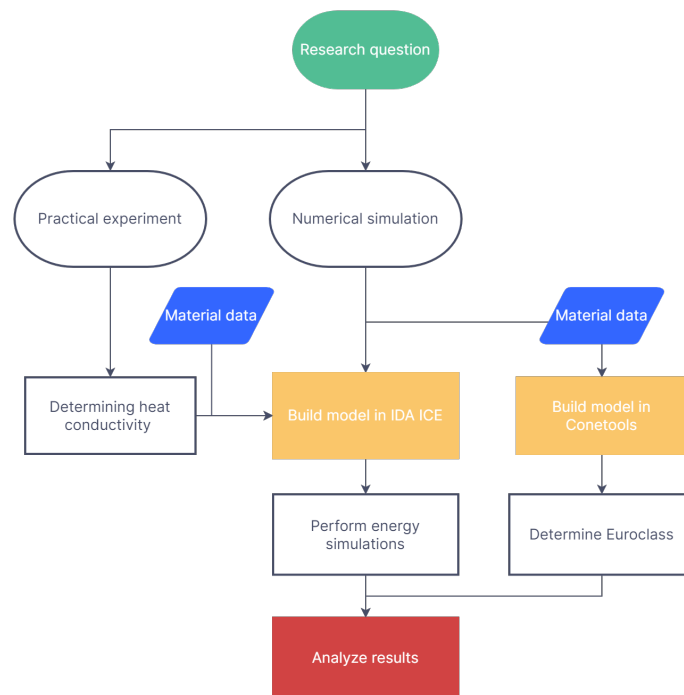


Figure 3.1: Flowchart of methodology

3.1 Climate room experiment

When researching the energy efficiency of the novel PCM, it was necessary to first gain knowledge of materials properties. This was done by utilizing a climate room located on the OsloMet campus to perform a steady-state experiment. The climate room allowed for a controlled experiment inside the confines of a controlled setting. The room consisted of two chambers: one for simulating the indoor environment, and a smaller chamber for simulating the outdoor environment. Further testing on the material was not done by the author but was instead supplied by the producer of the PCM, done through a Differential Scanning Calorimetry (DSC). In regards to the fire resistance

properties, no physical tests were performed by the author. An external cone calorimetry test was performed, and the raw data were received for further analysis.

Experiment design

Climate room setup

A 3D rendering of the laboratory can be seen in figure 3.2.

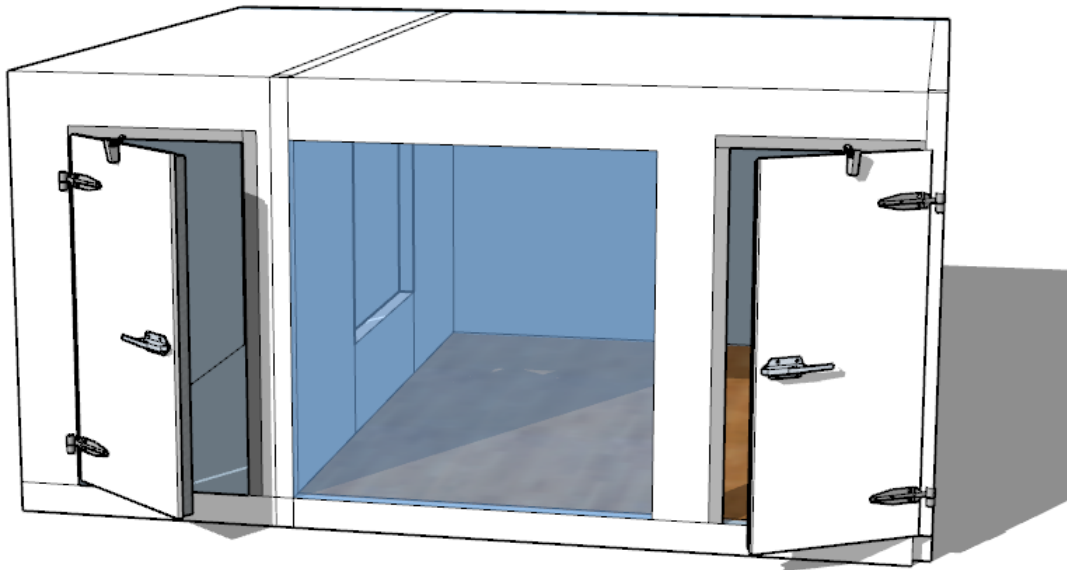


Figure 3.2: 3D rendering of the climate room setup

The test was performed in a well-insulated box located on the OsloMet campus. The box consisted of two rooms with different dimensions and a $(1.2 \times 1.2) m^2$ window connecting the two rooms.

Figure 3.3 shows the layout of the two connecting rooms, as well as the placement of the material. The larger room was used to simulate indoor temperature, while the small room was configured to keep a cold climate. The orientation in the figures is not representative of real compass directions, and is only used with the purpose to describe the climate room easier. This local system of orientation will be consistent throughout the rest of the report.

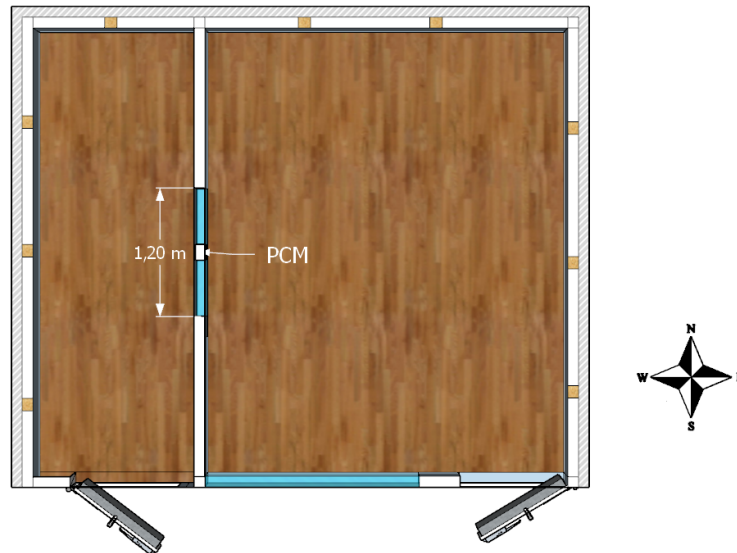


Figure 3.3: Plan view of the test room

The different components of the climate room were supplied by Fresvik AS as pre built components and can be seen in table 3.1. The technical report of the components can be seen in reference [19]

Table 3.1: Components of the building body

Element type	Structure	Thickness [mm]
Roof/walls	Steel sheet	0,7
	Polyurethane foam	100
	Steel sheet	0,55
Floor	Steel sheet	0,7
	Polyurethane foam	100
	Parquet	0.55

For the supply of fresh air, a dedicated air handling unit (AHU) is positioned just outside the room's east wall. An insulated duct and a diffuser in the room's center deliver the air, which is extracted at the southeast corner. The diffuser, which has a perforated face plate, spreads air horizontally in 360° approximately 30cm from the ceiling. The ventilation is set up as a mechanically balanced constant air volume (CAV). The user interface on the AHU was used to control the supply air temperature and airflow rates. For the experiment, the AHU temperature setpoint was 22°C. A sketch of the ventilation system in the room can be seen in figure 3.4.

The climate chamber's cold room had an air conditioning unit that supplied cold air into the space. Chosen set-point temperature of the AC unit was configured to 10°C, creating a preferable temperature difference on the materials surfaces. One thing that was not optimal in the experiment was the workings of the AC unit itself, as it did not supply the room at a constant rate. It had a tendency to switch on and off at a relatively high frequency. Although this was the case, this was not deemed a problem as the fluctuations did not show a huge effect on the surface temperature of the material.

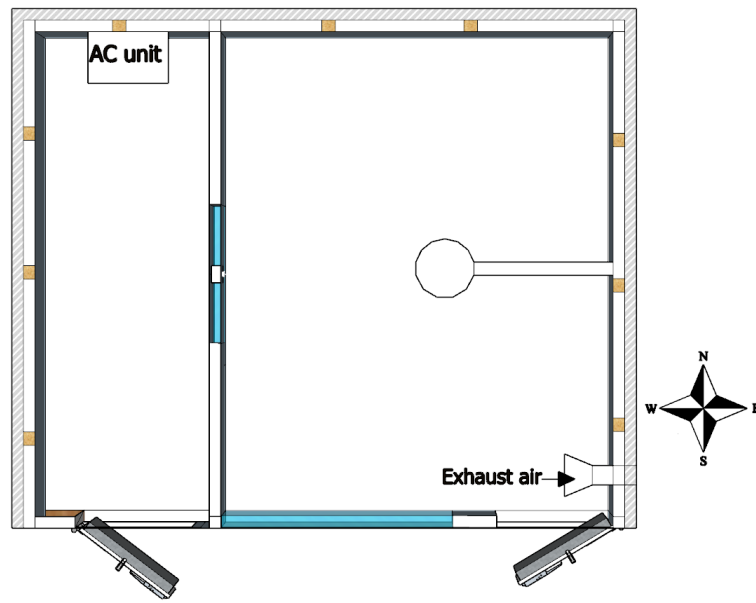


Figure 3.4: Ventilation and AC unit

Acquired material

The material used in the steady state experiment were created by applying the spackle in layers until a it reached the desired thickness. The sample had dimensions of $(15 \times 15)cm^2$, and a thickness of $2.1cm$. The total weight of the material was measured at $393.60grams$. A photo of the material can be seen in figure 3.5.



Figure 3.5: Weight of the PCM

3.2 Instrument principle and theory

This section will go over the measuring equipment and how they were utilized in the research.

Heat flux measurement system

Hukseflux TRSYS01 is a system used for on-site measurement in accordance to the standard practices of ISO 9869 [20], which is capable of measuring thermal resistance, R-value, thermal conductance, lambda value, thermal transmittance, and U-value of building envelopes.

The system is equipped with MCU01 electronics, two heat flux sensors of model HFP01 as well as two pairs of matched thermocouples of model TC. The sensors are used to measure at two locations. The two measurement locations provide redundancy, leading to a high level of confidence in the measurement result. The high accuracy of the heat flux sensors and temperature difference measurements ensures that TRSYS01 continues measuring when other systems no longer perform; in particular at very low heat fluxes and temperature differences across the wall. The TRSYS01 measures temperature differences with an uncertainty of better than 0.1 °C over the entire rated temperature range.

The HFP01 heat flux plates has a thickness of 5mm and a diameter of 80mm, with a guard ring made of a ceramic-plastic composition. HFP01 heat flux plates measures the heat flux density through the sensors itself, expressed in $[W/m^2]$. The sensor is a thermopile that measures the difference across the ceramic-plastic composite body of HFP01, by generating a small voltage that is a linear function of the temperature difference. The heat flux is proportional to the same temperature difference divided by the effective thermal conductivity of the heat flux sensor body. [21]

The TRSYS01 system connects to a logging software called "loggernet". While it's connected, it is possible to watch live graphs of all the different sensors. The device also stores average measurements over a 10-minute and 24-hour time period. Values from both heat flux sensors, thermocouples and temperature differences between the thermocouples gets collected. For this experiment, collected data over a 10 minute average value were used.

Intab PC-logger and thermocouples

Thermocouples are commonly used in a wide range of applications. It is made up of two distinct metals that are joined at one end. When the two metals' junction is heated or cooled, a voltage is produced that can be linked to the temperature. A thermocouple is a basic, reliable, and low-cost temperature sensor that can be utilized in a variety of temperature measuring applications. A photo of the PC-logger together with the type of thermocouple is shown in 3.6

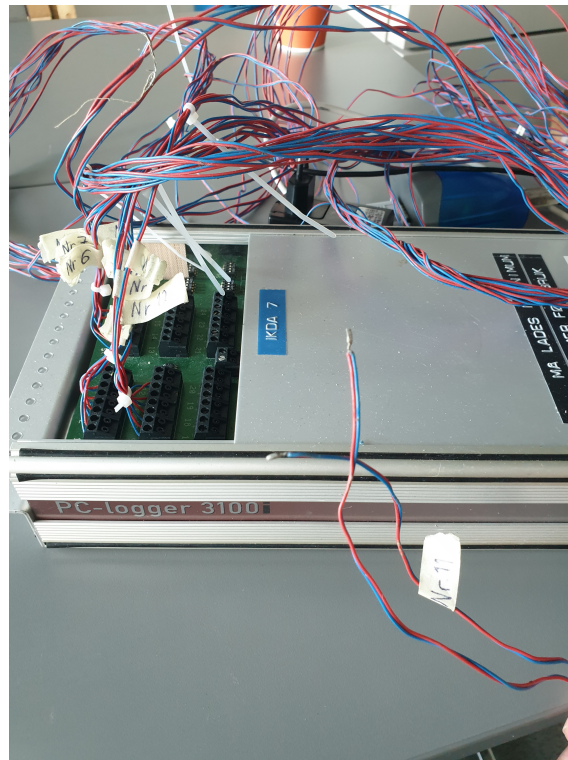


Figure 3.6: Intab-PC logger and thermocouple

Placement of the material

The first step in the experiment was to place the material in the window bridging the hot and cold room. As the size of the material did not fit the window, two $(60 \times 120)cm^2$ EPS blocks with a thickness of $10cm$ were used to fill the gap. Figure 3.7 shows how the EPS blocks were cut to fit the acquired sample. The EPS overlapped the material with approximately $2cm$ on each side to minimize airflow around the gaps. After the PCM had been placed, the whole thing were mounted in the window. Tape were also used on every corner of the material to further limit airflow after it was placed in the window.

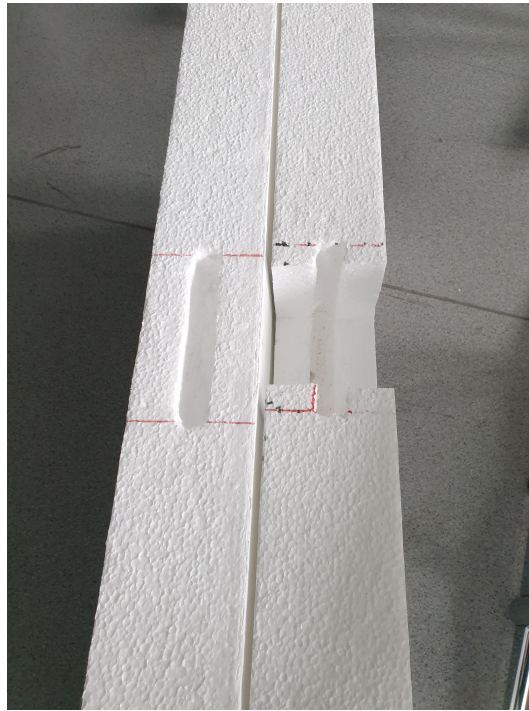


Figure 3.7: EPS blocks before inserted in the window

As instructed by the TRSYS01 manual, two thermocouples and a HFP01 sensor were mounted on both sides of the material using double sided tape. Although the size of the material were not ideal, it was just large enough that it could fit all the sensors. The matching thermocouples were place on the same spot but on opposite sides, allowing temperature difference to be measured at two separate location. A photo of the sensor placements for the hot side can be seen in 3.8, while figure 3.9 shows how the overall setup for both the warm and cold side of the material.

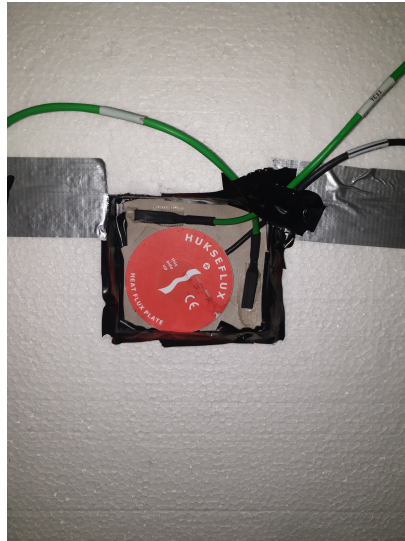


Figure 3.8: Placement of heat flux sensor and thermocouples, hot side



(a) Cold room



(b) Hot room

Figure 3.9: Photos of the two climate chambers

The placement of thermocoupled measuring air temperature can be seen in figure 3.10, and were logged at approximately 1.3m above the ground.

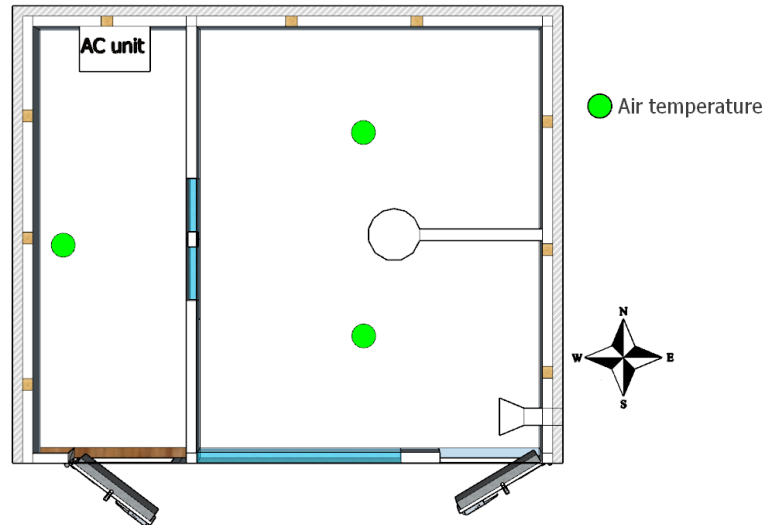


Figure 3.10: Location of air temperature measurement

3.3 Determining thermal conductivity

Thermal conductivity were calculated in accordance to ISO 9869:2014. The measurements itself didn't start before a couple of days had passed with both the AC unit and ventilation system switched on, and the two rooms had reached near steady state conditions. It was then measured for 72 hours. After a measurement period of 72 hours, the results were collected, analyzed, and confirmed to be in compliance of the standard.

Results gathered from the heat flux sensors and thermocouples were then used to estimates the materials thermal conductivity. This was done by using the measured heat flux, thickness, and temperature difference together with equation 3.1.

$$\lambda = \frac{\phi * d}{\Delta T} \quad (3.1)$$

3.3.1 Material properties

To use the PCM module in IDA ICE, additional data such as partial enthalpy and specific heat was needed. This is especially important when working with PCM, as its complexity and special properties can impact the end results. One of those important factors is thermal conductivity, which is obtained by the experiment mentioned earlier in this chapter. Additional information regarding the PCM was obtained through tests conducted by the PCM manufacturer. A differential scanning calorimetry (DSC) test was performed, allowing the heat capacity of the material to be determined. The DSC test is a common and powerful experimental technique for assessing thermodynamic properties in a substance [22]. Due to some complications in obtaining the data from this specific material, the same data used in Aamodt et al. were also used in this project. This was deemed to not be a problem since the material is from the same manufacturer,

and the values were expected to be of a similar range. An overview of the input properties used in IDA ICE can be seen in appendix A

3.3.2 Fire performance

A cone calorimeter test (CCT) was performed according to ISO 5660[23] at Lund University (Division of Fire Safety Engineering Faculty of Engineering, Lund University). The test is widely considered one of the most significant bench scale instruments for fire testing [24]. The Cone Calorimeter provides a wide range of data with a solid scientific foundation, allowing for a variety of applications. It can be utilized for both modeling and improved product development. By measuring oxygen concentration in the flue gases, the heat release rate of the specimen is calculated. This is because the heat released from the fuel has been shown to be proportional to the oxygen consumed during combustion. The results obtained from the cone calorimeter test can further be used in models for up-scaling experiments, and in fire testing when developing new materials [25].

The test method involves a test specimen within an area of 100mm x 100mm, which is exposed to a constant radiant heat flux. The heat flux can be adjusted from 10 kW/m² to 100 kW/m². A spark plug positioned over the test specimen ignites any flammable gasses produced by the test specimen. The effluents from the test is collected in a hood and transported through a duct. In the duct, there is a thermocouple, a pressure sensor, smoke measurement system, and a sample probe. Furthermore, the test specimen is positioned on a load cell, so the mass loss of the test specimen can be recorded during the test. The test equipment is show in figure 3.11

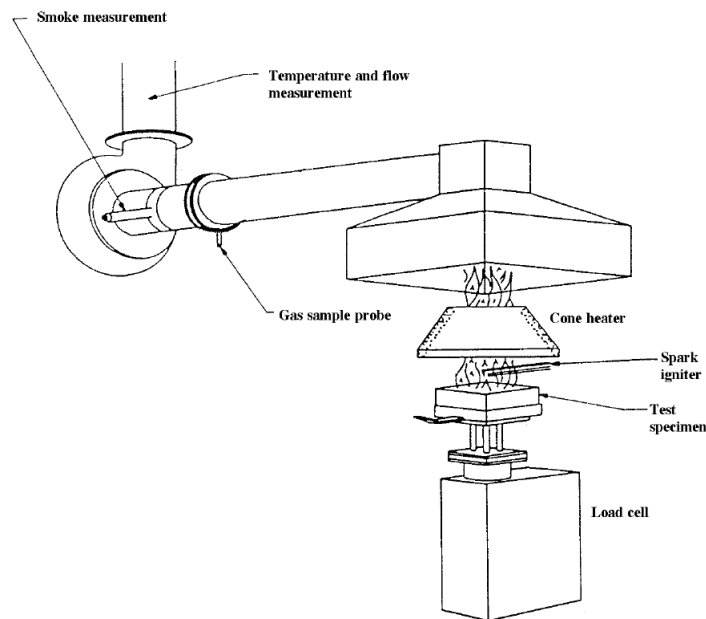


Figure 3.11: Cone calorimeter test

Conetools

Conetools is one of several flame spread models developed by RISE. It's a program that allows for the prediction of Euroclass for single burn item (SBI)[26], and room corner test (RCT), by utilizing results from a cone calorimeter test at one heat flux level. Using this program, one can circumvent the extra resources and time needed to perform a practical SBI and RCT. Not many studies were found validating the program, but the one that was found showed positive results. The program is not as accurate when studying heat release curves (HRR) curves, but is good at predicting the correct Euroclass [27].

3.4 Energy simulation

IDA ICE

IDA ICE was chosen as the simulation tool for assessing the building's energy performance and is a tool developed by the Department of Building Science (Stockholm)[28]. It's an innovative and trusted whole-year detailed and dynamic multi-zone simulation application for the study of thermal indoor climate as well as the energy consumption of the entire building. The program allows for full control over building parameters. It also covers a large number of building phenomena such as integrated airflow network and thermal models, vertical temperature gradient, CO₂, and moisture calculations. Most significantly, it includes a partial enthalpy mathematical model for PCM incorporation into the building envelope and internal structures.

Earlier studies showed that the PCM module IDA ICE outperformed similar simulation tools, such as TRNSYS and EnergyPlus [29]. The reason for this is that IDA ICE takes into account both the PCM hysteresis phenomena and the phase change temperature range. Validation of the PCM module in IDA ICE was also performed on a similar product from the same manufacturer [30]. The reported results concluded with a root mean square value error of 1.12% and a coefficient of determination of $R^2 = 0.976$, which indicated that the module had good predictive capabilities. The building model can be supplied by either synthetic or actual climate files, making it easy to select the preferred location of the building. Another reason IDA ICE was employed is due to the possibility of using different shading and window opening control methods through a graphical script.

3.5 Description of the building

The building itself were designed with the thought that the study should not limited itself to a specific layout or energy efficiency. As a result, a straightforward design constructed after the Norwegian building code's minimal energy requirements (TEK-17) were preferred. The building that was used in this thesis, is identical to the building used in an earlier study by Aamodt et al. A full compliance check of the building were performed using SIMIEN, as well as in IDA ICE. SIMIEN is a dynamic energy simulation software, with a module that checks the buildings TEK-17 compliance. The software checks the buildings total net-energy against the allowed budgets defined in TEK-17. This is done using defined values from the Norwegian standard, NS-3031, for climate, indoor setpoint temperatures, internal heat loads, and operating hours. For additional information on the validation procedure see citation[30]. The values are meant to standardize all buildings and serve as a common reference point for comparisons, not to represent realistic use of the building. For an overview of the main building components, see table 3.2. In the model exterior diffusive screens are set to be drawn when the facade experiences a solar radiation level of $100[W/m^2]$, this was done in order to get the net energy demand under TEK17.

Table 3.2: Building components

Material	$\lambda[W/mK]$	$\rho[kg/m^3]$	$Cp[J/kgK]$
Concrete	2300,0	1050,0	1,7
Insulated wooden frame wall	92,0	2010,0	0.052
Insulation	20,0	750,0	0.036

3.5.1 Office cubicles

It was decided not to model the entire structure when performing energy simulations, but instead only one section of the building. This was to save time, as it would take a considerable amount of time to run each simulation with a building of that size. The section can be seen in figure 3.12 The office space is on the third floor, against the south wall. Multiple cubicles and a long corridor make up this portion. All cubicles in the simulation are modeled after guidelines published by SINTEF Byggforskserien [31]. The total floor area of this section was $636m^2$, with a volume of $1084,4m^3$. For more information about the simulated area, see appendix B.

Table 3.3: Building materials in IDA ICE

Material	rho kg/m3	Cp J/kgK	lambda W/mk
Concrete	2300	1050	1.3
Chipboard	1000	1300	0.13
Wood	500	2300	0.14
Insulated wooden frame wall	92	2010	0.052
Gypsum board	970	1090	0.22
Light insulation	20	750	0.036

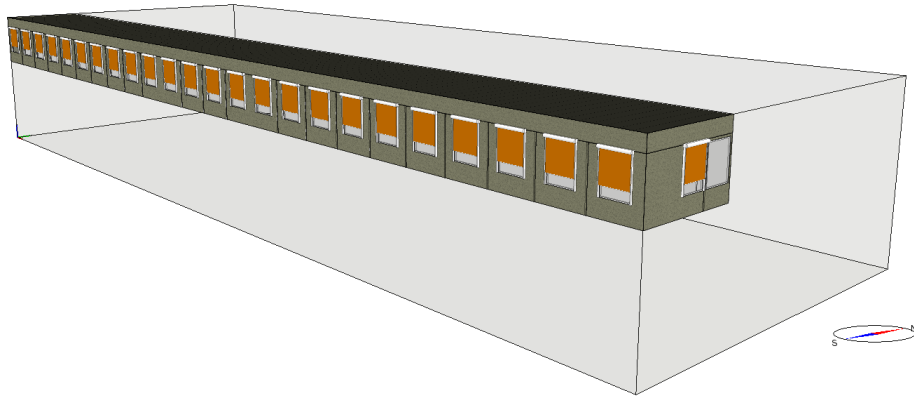
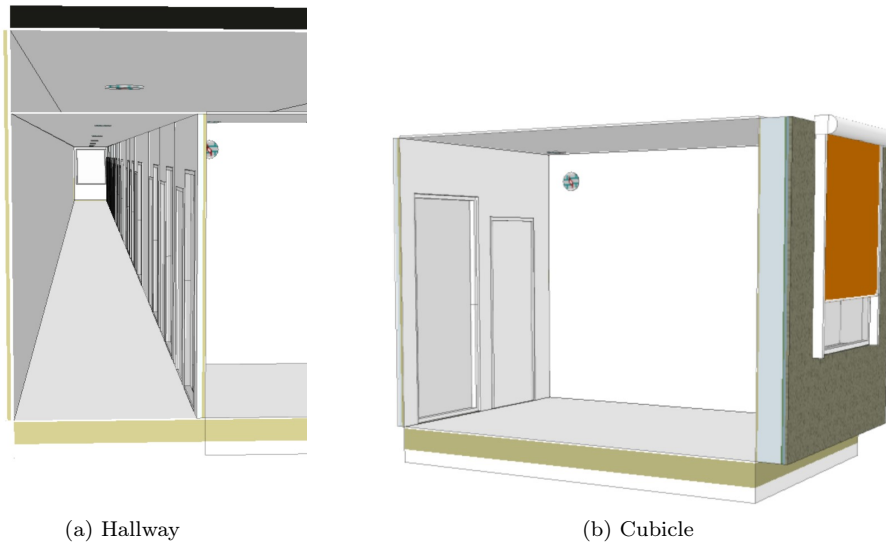


Figure 3.12: Section of building used for simulation



(a) Hallway

(b) Cubicle

Figure 3.13: Model of the hallway and one cubicle in IDA ICE

Standard values were used when inserting the internal heat gains generated inside each cubicle and hallway, and can be seen in table 3.4.

Table 3.4: Internal gains

Space	Internal heat gain	Value	Schedule	Weekend
Cubicle	1x Occupant	1.2 Met	08:00-18:00	Off
	1x Light	60 W	08:00-18:00	Off
	1x Computer	60 W	08:00-18:00	Off
Hallway	8x Light	102 W	08:00-18:00	Off

The CAV schedule and airflows is shown in table 3.5. The inputs are based on the minimum requirements after TEK-17's air quality requirements for office spaces. The ventilation rate for the hallway uses the same minimum requirements, with $2.5 \text{ m}^3/\text{h} * \text{m}^2$ during the occupied hours and $0.7 \text{ m}^3/\text{h} * \text{m}^2$ the rest of the time.

Table 3.5: Cubicle CAV schedule

		CAV airflows			
		m3/h·m2	m3/h		
	Min	0.7	6.32		
	Max	5.4	48.6		
	During NV	OFF			
		Weekday			
		00:00-07:00	07:00-18:00	18:00-21:00	21:00-24:00
Reference case	Min	Max	Min	Min	
Without PCM	Night ventilation	Max	Min	Night ventilation	
With PCM	Night ventilation	Max	Min	Night ventilation	
		Weekend			
		00:00-07:00	07:00-18:00	18:00-21:00	21:00-24:00
Reference case	Min	Min	Min	Min	
Without PCM	Night ventilation	Min	Min	Night ventilation	
With PCM	Night ventilation	Min	Min	Night ventilation	

3.5.2 Climate

The outdoor climate used in all the simulation were located in Oslo, Norway. The EPW file that was imported directly to IDA ICE were created from the data collected at the weather station at Blindern. The climate has an classification of Dfb according to the Köppen climate classification [32]. The weather file itself is constructed after EN-ISO 15927-4 with data from 2003-20013 [33].

The file contains multiple important variables needed for a correct energy calculation, such as dry-bulb temperature, direction of wind, direct normal radiation form the sun etc. One of the things that was taken into account when choosing a simulation time-slice were temperature, as it was desired to use the month with the highest mean temperature. Figure 3.14 shows that the month of July had both the highest peak temperature, as well as highest mean temperature. Using another month would likely change the overall results, as the change in cooler ambient air temperature would increase the effectiveness of night cooling. An example of this would be that the amount of air needed for effective cooling during the month of August would be considerably lowered, as the average temperature at night and heat gain during the day is less.

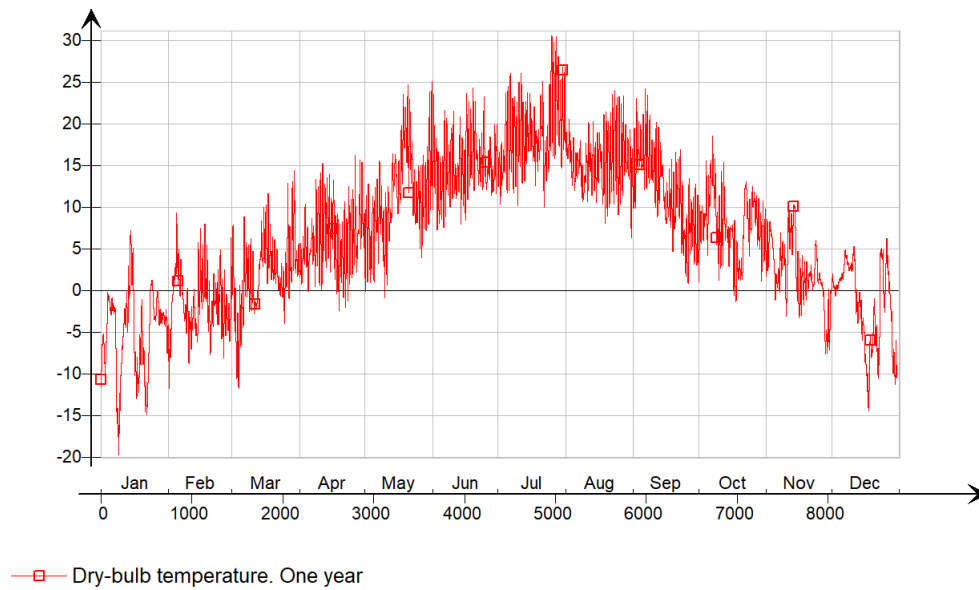


Figure 3.14: Temperature variations, one year

3.6 PCM energy performance

One of the more interesting energy saving strategies is utilizing passive cooling, which is techniques maintaining comfort without the use of mechanical refrigeration. By using the buildings structure and its ability to store thermal energy, passive techniques can show huge improvements in terms of thermal comfort and energy use. By utilizing PCM, aspects of passive cooling will hopefully be enhanced. This section will focus on the different parameters that will be used in combination with the novel PCM.

3.6.1 Increasing PCM effectiveness using night ventilation

Night ventilation (NV) is a passive cooling technique in which a building's daytime heat gain is discharged at night through the intake of cool external air. The intake of cold air circulates through the building, resulting in cooling down the buildings structure. This process will in turn decreases the rate at which the internal temperature rises during the day [34][35]. As a consequence of cooling the building at night, the cooling energy demand needed for the buildings operative temperature to be within comfortable temperature during the day will also decrease. A research into night ventilation showed that there are some key parameters linked to its efficiency [36]. The parameters that were identified were the relative difference between indoor and outdoor temperature at night, the ventilation effectiveness at night, and the thermal capacity of the building (which will be increased by applying PCM spackle) . Using the ambient air as a heat sink to decrease temperature during the night plays a significant role when working with PCM. One of the focuses will be to lower the temperature to the point that the the material changes phase, and therefore gets utilized close to its full potential. How this will be monitored is described in a later section.

When cooling the building using natural ventilation, it was desired to control the window openings to the point where a specified ACH could be obtained. The first thought were to use a

simple PI controller that signaled the windows to open a certain degree during the night. This solution presented to be problematic since airflow through an windows is affected by a number of variables, including wind speed, pressure difference and air temperature difference inside and outside. As a result, the ACH for the cubicles and hallway were less stable than desired.

The solution that was used instead, was to utilize a zone controller macro that monitored total inflow and outflow of all windows in a zone. The windows would then regulate window openings until the desired ACH in the room were achieved. A screenshot of the macro configure with a maximum of 3 ACH can be seen in 3.15. The macro is also set to not let the individual zone temperature go below 19°C. Time schedule for the windows were set to operate between 21-7 every night.

The result file for both 3 ACH and 5 ACH can be seen in figure 3.16 and 3.17, together with the in-signal recorded from the output file. Note that the L/s is not a perfect straight line, which is again contributed to the multiple variable that control in- and outflow.

To check if the macro worked as intended, the data from the 5 ACH simulation were imported to excel for a closer inspection. The data containing air flow through the external window were logged for one cubicle, during two separate nights. The airflow had an average value of 33,718 and 33,711 L/s, which calculated to 4,996 ACH in the zone for both nights.

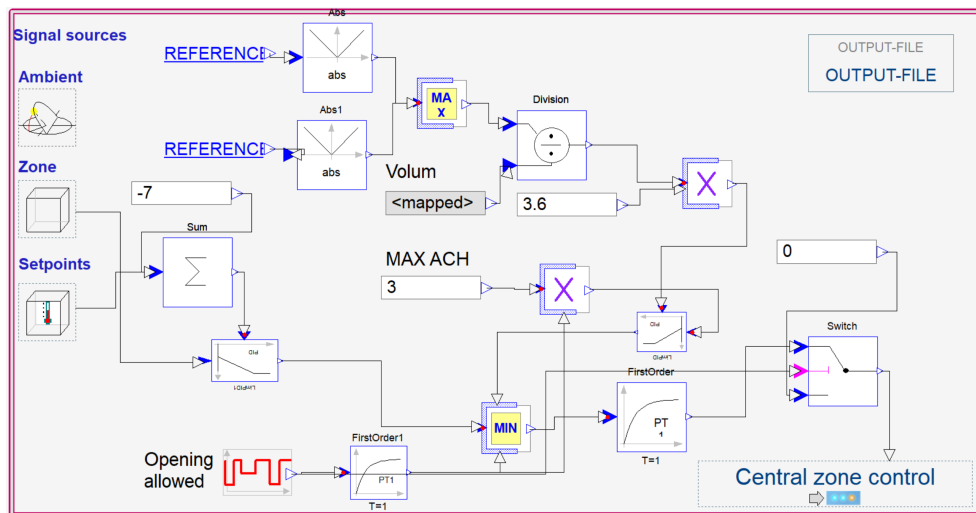


Figure 3.15: Night ventilation macro

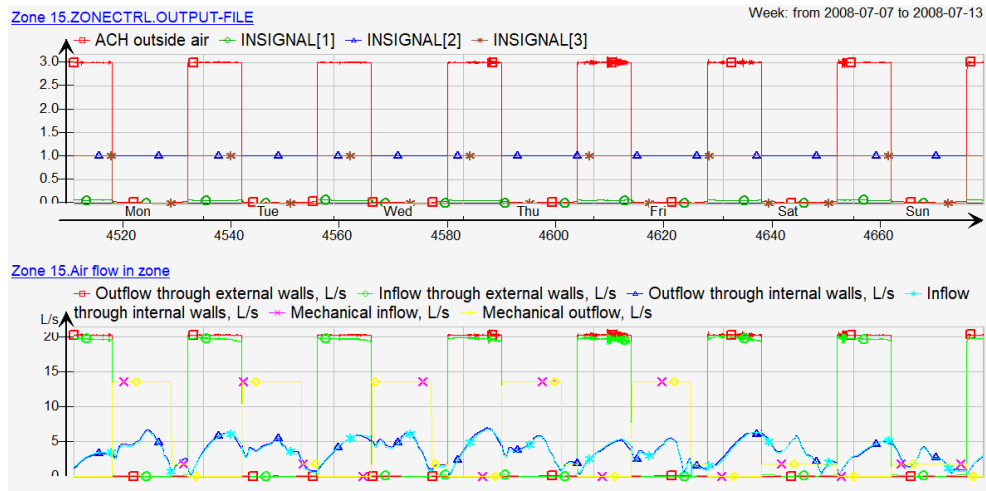


Figure 3.16: 3 ACH

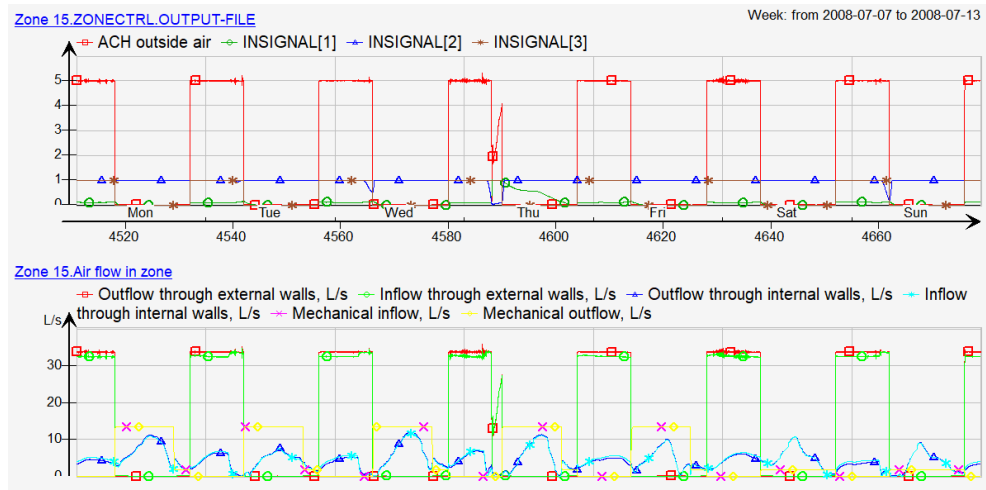


Figure 3.17: 5 ACH

3.6.2 Solar shading

The key reason for installing a shade device is to prevent direct sunlight and solar radiation from entering the structure during the cooling season, while also allowing for desired solar gains during the heating season[37]. There is however a difference between exterior and interior shading. When solar shading devices are installed on the exterior, they can effectively filter solar radiation before it passes through the window glass. Far-IR radiation from the interior surfaces, on the other hand, cannot pass through the glass when the shading device is mounted to the interior. As a result, the heat is trapped inside the structure. During an overheating period, this can lead to an increase in cooling loads[38]. An extensive research were conducted by Rabani et al. where he looked into multiple variables for achieving zero-energy building performance, including multiple types of solar shading parameters. The research included multiple variations of shading material

types, coupled with different control mechanisms for when the shadings were drawn. According to this research, venetian blinds were one of the more optimal shading materials[39]. Shading will also play an important part of passive cooling with PCM and delaying the peak temperature. If the PCM collects too much thermal energy during the day, there will be a higher probability that it fails to solidify during the night. This will in turn make the next day prone to higher temperatures and cooling loads. The additional shading device that will be used is venetian blinds, an illustration of the blind can be seen in 3.18 Considering the time frame of this time-bounded work, only two different types of solar shading materials will be investigated, and how they both influence the energy performance of the PCM. Information regarding the material properties can be found in appendix C

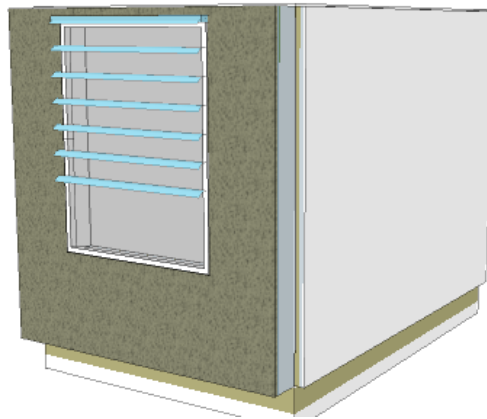


Figure 3.18: Cubicle fitted with venetian blind

3.6.3 Simulation cases

During the first 30 simulation cases, only two parameters were changed, namely different ACH during night ventilation coupled with multiple variations of PCM thickness. After this, another 30 simulations were performed with venetian blinds. An overview of the different settings that were changed during the simulations can be found in table 3.6, note that this does not include changes in the CAV schedule as this is explained in table 3.5. The ACH in the table references the the amount of air changes per hour caused by the supply of fresh air through the windows for each zone. All the interior walls and ceilings of the cubicles are varied with the same amount of PCM for each case.

Table 3.6: Night ventilation and PCM variations

	ACH	PCM spackle [mm]	Shading type
Reference building	No night ventilation	No PCM	Screen, Blind
Cubicles without PCM spackle	2,3,4,5,6	No PCM	Screen, Blind
Cubicles with PCM spackle	2,3,4,5,6	2,3,4,5,6	Screen, Blind

3.6.4 Energy efficiency calculations

With the purpose of calculating the overall energy use of the building, all energy systems were given a coefficient of performance (COP) of 1. This change would allow the results to show the true energy usage of the components, and not values dependant on individual COP. Different cooling units used to cool the room would therefore use the same amount of energy based on the amount cooling delivered. This includes the CAV with a set-point temperature of 19°C. Since the window are set to close when it reaches 19°C, there were no need for any form of heating other than the AHU. Specific Fan Power (SFP) for the supply and exhaust fans were given a value of $1.5kWh/m^3/s$ and $1.0kWh/m^3/s$, respectively.

TEK17's building code regarding indoor climate has some set values when it comes to minimum and maximum temperatures to ensure thermal comfort. The summer conditions of a standard office building where the people inside are only doing light work, must not exceed 26°C over 50 hours per year. To ensure that the building is still in compliance with this, the model has an unlimited ideal cooler unit in every zone of the office space with a set-point of 26°C. The coolers are not meant to represent a real life cooler, but as a tool to remove all the excess heat in the zone. The COP of 1 makes it comparable to other cooling alternatives.

Local cooling reduction

When evaluating the results from the multiple simulations, one of the things that were noted were how much the building used by the mechanical cooler at zone level. The cooling loads were calculated for the entire building, and put in equation 3.2 to get a comparison with the reference building. The output were then the difference in percentage.

$$E_{saved} = \frac{E_{ZoneCooling,reference} - E_{ZoneCooling}}{E_{ZoneCooling,reference}} \times 100[\%] \quad (3.2)$$

Total energy reduction

The mechanical cooling is however not the only energy post being effected by the difference in strategies. There will also be a difference in energy used in the air handling unit, as well as fan usage, as the AHU will be shut off during NV. To find this result equation 3.3 was used. " $E_{Electriccooling}$ " refers to the amount of electricity spent on both mechanical cooling units as well as AHU

$$E_{saved} = \frac{E_{Electriccooling+fans,reference} - E_{Electriccooling+fans}}{E_{Electriccooling+fans,reference}} \times 100[\%] \quad (3.3)$$

3.6.5 Solidification of the PCM

In order to observe that the PCM is being used to its potential, it would be interesting to keep track of whether or not it went through a phase transition. The temperature criteria for the PCM to achieve solidification were determined to be at 20°C, as seen by the DSC test. One of the standard results obtained with IDA ICE is the surface temperature of all interior surfaces. However, because this temperature does not reflect the material as a whole, it was determined that it would not accurately represent the PCM temperature. IDA ICE provides a tool that allows the user to delve into the building construction and log temperatures at multiple points. This allowed for temperature to be recorded in between the PCM layer and the gypsum. The reasoning behind this choice is based on the assumption that if the most inner part of the PCM layer has reached 20°C, the rest of the layer has likely reached that temperature as well. Figure 3.19 shows a visualisation of the IDA ICE model, with the point of logged temperature.

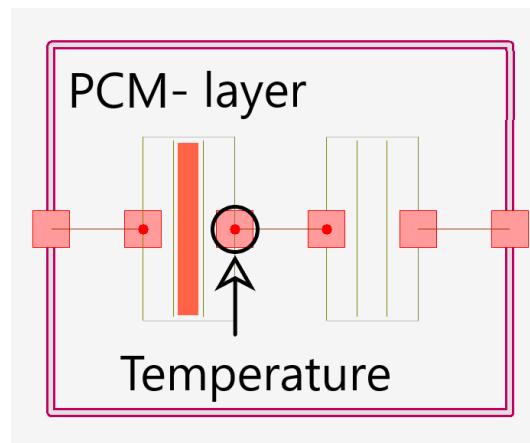


Figure 3.19: Point of logged temperature

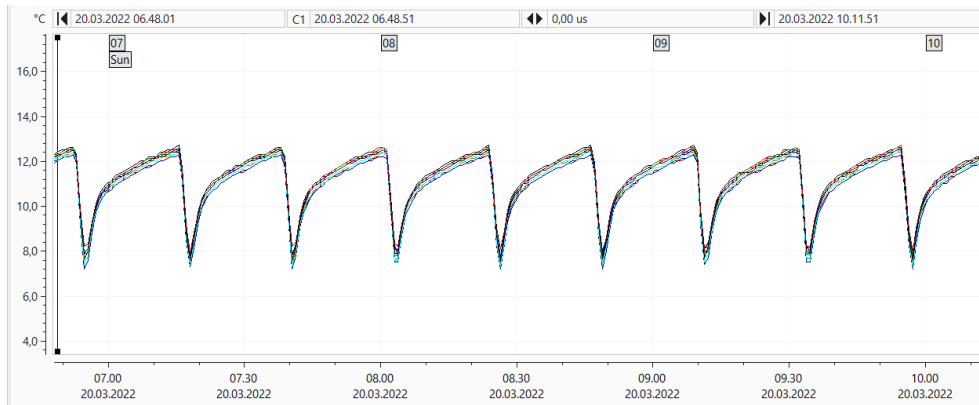
4. Results and discussion

This chapter will present results gathered from both the practical experiments, and the numerical simulations. This will include analysis of data and discussion of the results.

4.1 Steady-state experiment

Data collected from the climate room experiment were logged over a 72-hour period, as per instructed by the ISO standard. The air temperature for both rooms was measured with two different Intab PC-loggers and can be seen in figure 4.1. Note that the internal clock on the PC-loggers was not set up, so the date and hour of the day do not reflect real data. The graph related to the cold room only shows a small time slice, and was done intentionally to get a closer look at the temperature variations. The same variations consisted through the entire experiment. The temperature of the hot room displays the whole experiment period.

The temperature in the hot room was supposed to stay consistent, but showed to have a small increase in temperature over the testing period. What caused this unwanted variation is unclear, but is highly likely to be connected to changes in the ambient environment. This variation was however not deemed to impact the end results.



(a) Measured air temperature in cold room



(b) Measured air temperature in hot room

Figure 4.1: Measured air temperature

A screenshot from the Hukseflux measuring device can be seen in appendix D. It depicts data gathered from the two heat flux sensors, as well as the four thermocouples. The figure shows the 10 min average of the heat flux sensors, surface temperatures from the thermocouples, as well as the surface temperature difference between the two thermocouple pairs. "HF1" and "HF2" are values collected by the heat flux sensors, from the hot and cold side respectively. "T11" is the mounted thermocouple on the hot side, and "T21" is mounted on the cold side. "DT1" and "DT2" represent the temperature difference between the two thermocouple pairs. Note that all the data in the graphic result should be considered as absolute values.

As seen in the plot, the sensors mounted on the cold side varied quite a lot. This is due to the fact that the cold chamber used an air conditioner that did not hold a steady flow of air, but instead turned on and off when the room temperature deviated with ca. $\pm 2.6^{\circ}\text{C}$ away from the set-point of 10°C . Resulting in both big air velocity variation as well as fluctuating temperature conditions.

The average value collected over the three days the experiment was running can be seen in table 4.1

Table 4.1: Results from TRSYS01 sensors

DT1 [K]	DT2 [K]	HF1 [W/m ²]	HF2 [W/m ²]	Thickness [m]
6,15	5,35	26,05	24,82	0.021

By using these results together with equation 3.1. The PCM's average heat conductivity was calculated to be $k \approx 0.093 \frac{W}{m \times K}$. And is comparable with earlier findings regarding a similar material. Gyproc also estimated a value of 0.1 for the sample used in [30].

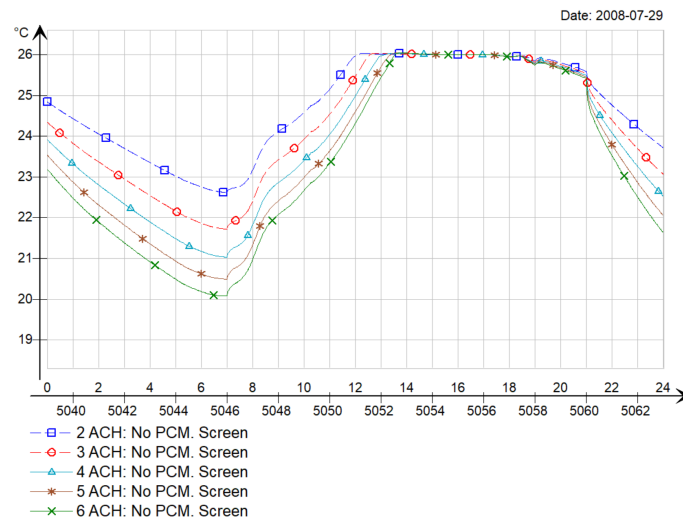
4.2 Numerical simulations

The results from the numerical simulations will be presented in this section. All IDA ICE simulations were performed during the hottest month of the year, July. When presenting temperature variations, a cubicle in the center of the building is often used, but results connected to energy usage will include the entire section of the building. The main parts of this chapter will be to first look at each individual passive cooling technique, and how it affects the building. The energy analysis will first be performed on the mechanical cooling, and ignore the total energy used for the building. The mechanical cooling load will in a way represent the extra energy that was necessary to introduce into the building on top of the ventilation. Total energy reduction will then be analyzed and will include the total energy posts affected by the measures.

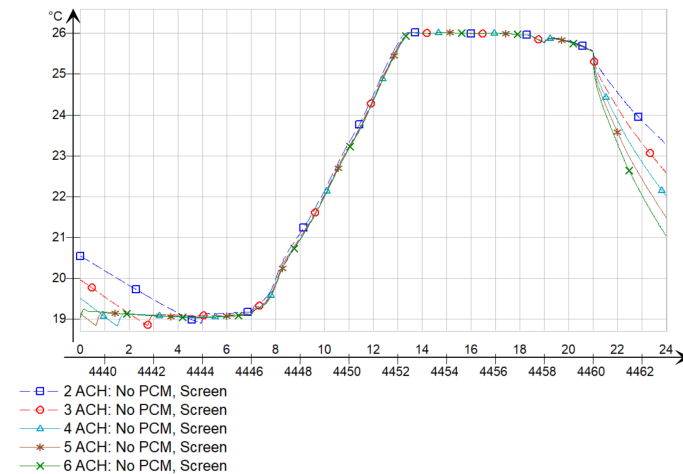
4.2.1 Effect of different parameters

Effects of night ventilation

As mentioned earlier in the thesis, night ventilation as a concept has been shown to have a positive effect on indoor temperature even without the use of PCM. This was also true for this office building 4.2(a). When raising the effectiveness of night ventilation during the night, it took a longer time for the temperature in the cubicle to reach 26°C. However, during nights that had a relatively low ambient temperature, the need for higher airflow became unnecessary. Figure 4.2 (b) shows an example of this. Although some of the earlier research conducted on this topic has shown that lowering the set-point of the night ventilation can give favorable results, this was not done in this thesis. The reasoning being that this could create an unfortunate event where the temperature at the start of the day would be below 19°C, which in turn would create extra energy usage in terms of zone heating.



(a) NV set-point temperature not reached



(b) NV set-point temperature reached in all cases

Figure 4.2: Operative temperature development created by NV

Effects of shading

As a large portion of the building facade contained windows, solar flux contributed to a considerable amount of the thermal energy gained during the day. As a consequence, the thermal rise in the cubicle was accelerated. This is evident from looking at the operative temperature after changing the screen shading material with a more effective material such as venetian blinds with a constant slat angle of 45° . This can be seen from the delay of peak temperature in figure 4.3. Even though the operative temperature at the start of the day was differentiated by ca 1.5°C , the case where blinds were used reached peak temperature at a later point. This gives a clear indication that the venetian blinds were more effective at minimizing solar heat gain, and halting the thermal rise of the cubicle

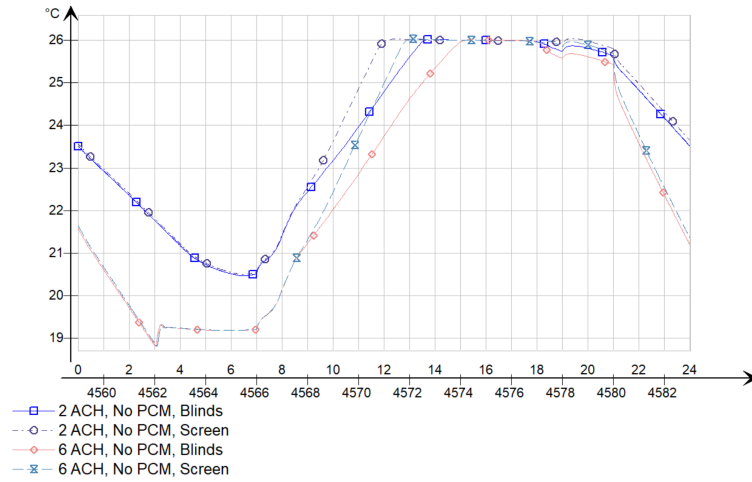


Figure 4.3: Temperature development caused by different shading material

Effects of PCM thickness

Figure 4.4 shows an example of 5 different simulations with the same amount of ACH at night. The difference in each case is the amount of PCM applied to all interior walls and ceilings, varying from 2mm to 6mm . Even though the operative temperature in all simulations started at approximately the same temperature, the thermal development during the day was different for each case. Having only a layer 2mm applied on the interior gave the highest temperature peak, while the case with the lowest temperature peak had 6mm applied.

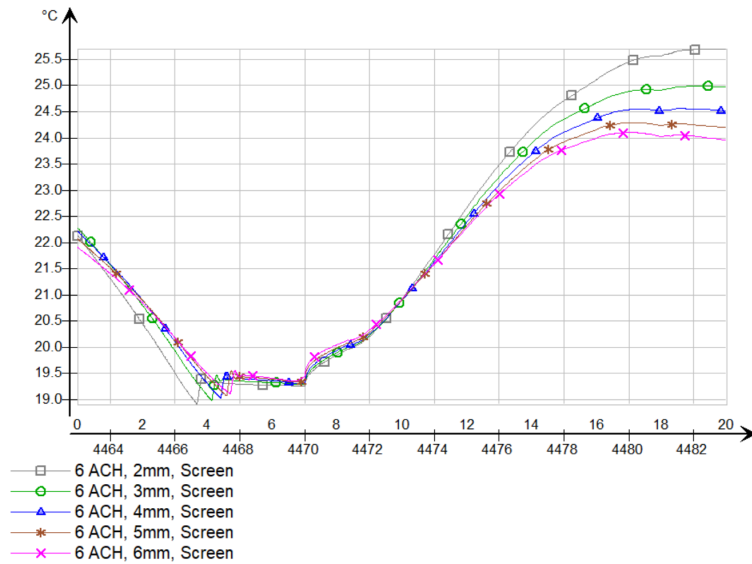


Figure 4.4: Effects of PCM thickness on operative temperature

Figure 4.5 shows a cubicle's operative temperature variation during a 24-hour period. Although the day before had cooling activated, the highlighted day had no mechanical cooling with the intention to present the full range of temperatures. Temperature differences during night and day were greatly affected by PCM thickness. The cubicle with no PCM applied had a total temperature difference of 9.54°C , while the case with the thickest amount of PCM only had a difference of 6.25°C . Almost all variations of PCM thickness reached 26°C at the same time, which occurred as a result of the ambient temperature being too high during the night. This illustrates a problem that can occur when PCM and high temperatures limit the night ventilation's abilities to cool the building. Having too much PCM applied could possibly give a negative impact, and requires the need for higher airflow rates during the night to fully release the saved thermal energy gained during the day. This figure can give an insight into why diminishing returns occur at higher layer thicknesses.

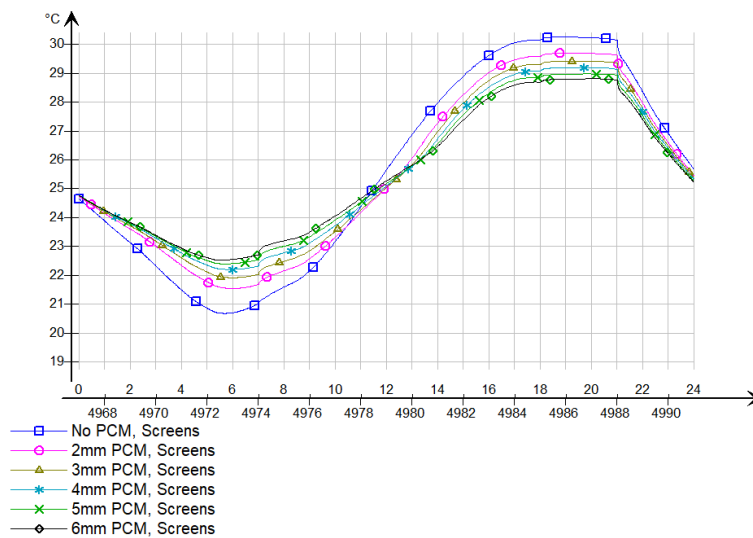


Figure 4.5: Diurnal variation

Effect of the PCM on temperature peak shift and energy peak load

In Norway, TEK-17 gives clear requirements regarding operative temperature limits for the typical office building. The temperature is not to exceed 26°C for more than 50 hours per year. What occurs when this value is about to be reached, is that measures must be taken to halt the increase in temperature. Sometimes this requires the implementation of extra cooling units, which was also the case for the simulated building. By effectively delaying the time it took for the temperature to reach 26°C with the use of passive cooling techniques, the amount of energy used on electric cooling decreased.

As shown earlier, by applying a PCM layer on the surface of all interior walls and ceilings, there is a notable difference in temperature development. Figure 4.6 shows a comparison of 6 different simulations with a night ventilation setting of 6 ACH. At this date, the use of PCM prevented the temperature from ever reaching 26°C , effectively removing 100% of the energy spent on mechanical cooling.

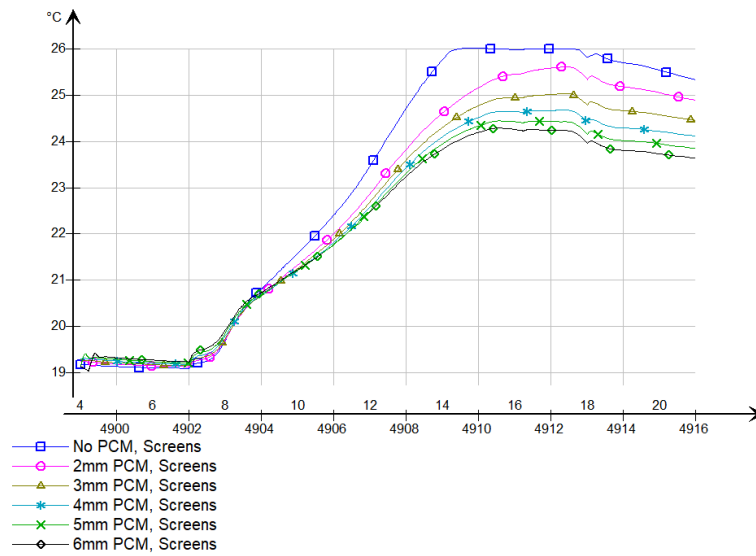
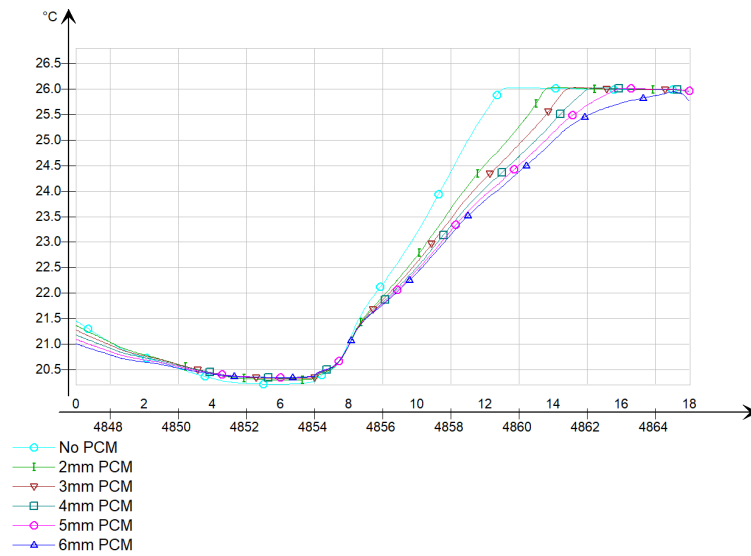
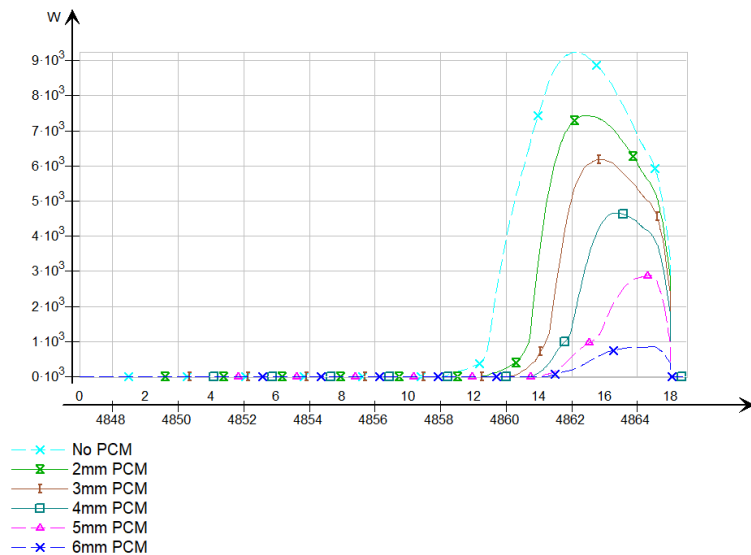


Figure 4.6: Temperature peak reduction

To show how the electric cooling load is connected to temperature peak delay, two graphs from the same day are shown in figure 4.7. All cases reached the set-point temperature, which means that every case had to use extra energy to not exceed 26°C. The peak load and total energy spent, on the other hand, were substantially different. The amount of energy spent decreased as more PCM was applied, as well as the peak load occurred later in the day. Although this figure does not represent the whole month, it gives a good indication of how the two results are connected.



(a) Operative temperature

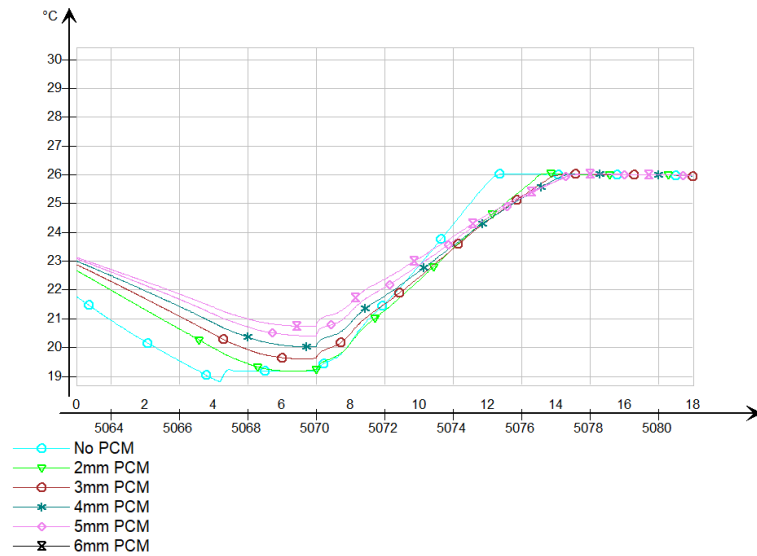


(b) Cooling load

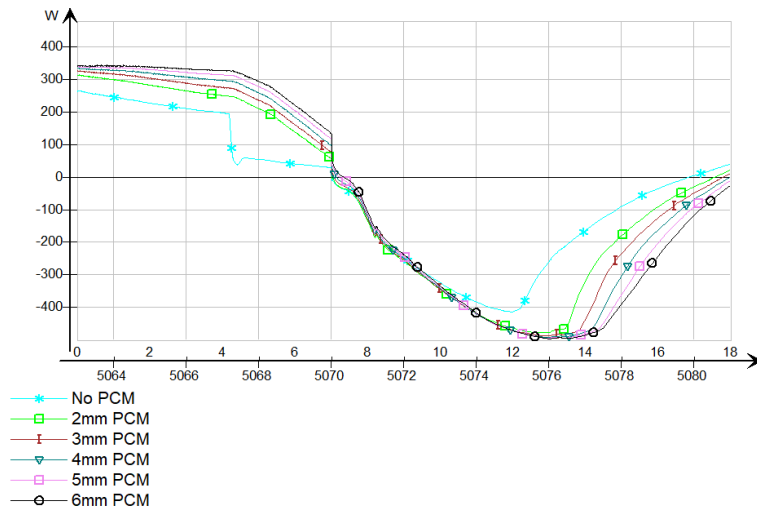
Figure 4.7: Correlation between temperature peak delay and cooling load

The graph above showed how the cooling load was decreased by delayed peak temperature. But even on days where there was only a small peak delay in temperature, PCM still gave benefits in regards to the cooling load. This can be shown in IDA ICE as the program calculated the energy balance of every cubicle. Figure 4.8 shows the temperature and energy balance for a day that reached peak temperature at approximately the same time. By looking at the heat balance in the room, specifically the heat balance of interior walls and masses, the positive effects of PCM can be seen. The PCM continued to absorb substantial amounts of energy even after peak

temperature was reached, effectively lowering the amount of energy that needed to be extracted by the mechanical cooling unit.



(a) Operative temperature



(b) Room heat gain caused by walls and masses

Figure 4.8: Correlation between PCM thickness and room heat gain.

4.2.2 Energy analysis

Local cooling reduction without PCM

The first results will focus on how the local cooling is affected by night ventilation and shading material alone.

Impact of night ventilation

Night ventilation had a big impact on the local cooling load, even without the application of PCM. Table 4.2 summarizes the amount of energy used in comparison to the same building without NV. The lowest setting of 2 ACH gave a total of 42% reduction, with every increase in ACH giving diminishing returns. The reason for this was because of the relatively high cooling set-point temperature of 19°C. This set-point was reached quite frequently in all cases, as low amounts of ambient air were enough. With only a few nights benefiting from the increase in ACH. For months with lower average night temperatures, higher ACH would most likely be unnecessary.

Table 4.2: Cooling load reduction by night ventilation having screen shading

Case	kWh	Reduction
Reference building	1476	Reference
2 ACH	849	42 %
3 ACH	706	52 %
4 ACH	634	57 %
5 ACH	591	60 %
6 ACH	570	61 %

Impact of night ventilation with venetian blinds

The impact created by the change in shading material alone reduced the building's local cooling load by 30%. Increasing the airflow resulted in the reduction of local cooling in both cases, but showed to have less impact in the building with blinds. This was caused by the thermal energy gained during the day being generally lower with blinds, which in turn made it easier for the indoor temperature to reach the 19°C set-point temperature at night.

Table 4.3: Cooling load reduction with external blinds

Cases	kWh	Total difference
Reference building	1476	Reference
Reference building w/ blinds	1026	30 %
2 ACH	473	68 %
3 ACH	360	76 %
4 ACH	304	79 %
5 ACH	272	82 %
6 ACH	256	83 %

Local cooling reduction with PCM

Ventilation rates in the building followed TEK-17 requirements for minimum airflow, as well as used a common set-point of 19°C during summer conditions in Norway. However, this was insufficient to keep the cubicles cool enough to fulfill the maximum temperature limit, necessitating the addition of mechanical cooling units in each room. Like the results shown above, these results depict the energy used only by the mechanical cooling units and will give an understanding of the additional energy required for each case.

Figure 4.9 shows the percentage of local cooling that was reduced compared to their respective building. Both the building with screens and the same building with blinds had local cooling loads of 1476 kWh and 1026 kWh, respectively. In both cases, it was clear that the use of PCM created an impact on the local cooling load. Some simulations were also done using PCM without NV, but as the cooling load was only reduced by less than 1% it was not included in the report. Without NV, the PCM was unable to dissipate the stored heat and hence had no effect.

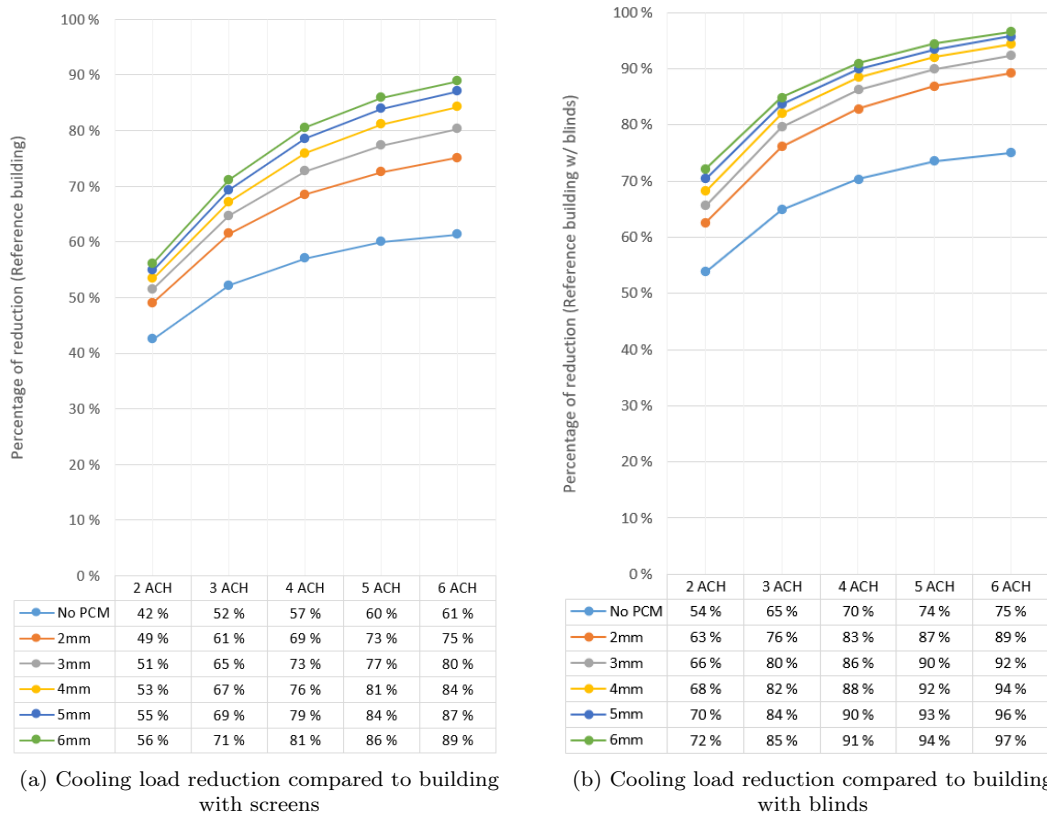


Figure 4.9: Local cooling load reduction of both cases

As seen in figure 4.9 (a) only using night ventilation reduced the amount of cooling considerably, it did however stagnate at higher values for reasons mentioned earlier. When introducing PCM to the building, the impact of night ventilation was amplified with every increase of ACH. The building's thermal heat storage capacity increased when the novel PCM spackle was applied

to its interior surfaces, while simultaneously benefiting more from increased night cooling as more energy was required to be removed.

Figure 4.9 (b) shows the same simulation cases, but with exterior blinds on the windows instead of screens. With the building having blinds installed, a reduction in the cooling load caused by PCM could also be seen. There were however some differences that emerged between the cases, More PCM had a bigger impact on low ACH while having less impact on high ACH. As the only difference between the cases was shading devices, must mean that this is caused by the change in solar heat gain.

The overall impact created by changing shading material, introducing NV, and applying PCM is shown in figure 4.10. Some cases came close to removing 100% of the 1476 kWh local cooling load, while over half of the cases reduced the load by 90% or more. In these comparisons, it is clear that the increase in thickness is not the key factor for lower energy consumption. Rather, the key variable is having enough night ventilation. The results show that the reduction above 4 ACH is minimal, and can possibly be regarded as unnecessary. The overall application this could mean for a real building is the cost reduction it produces. Not just by using less energy for cooling, but by never having to install any form of local cooling devices. The few instances that need additional cooling can possibly be dealt with by lowering AHU temperature or increasing the airflow rate of the ventilation.

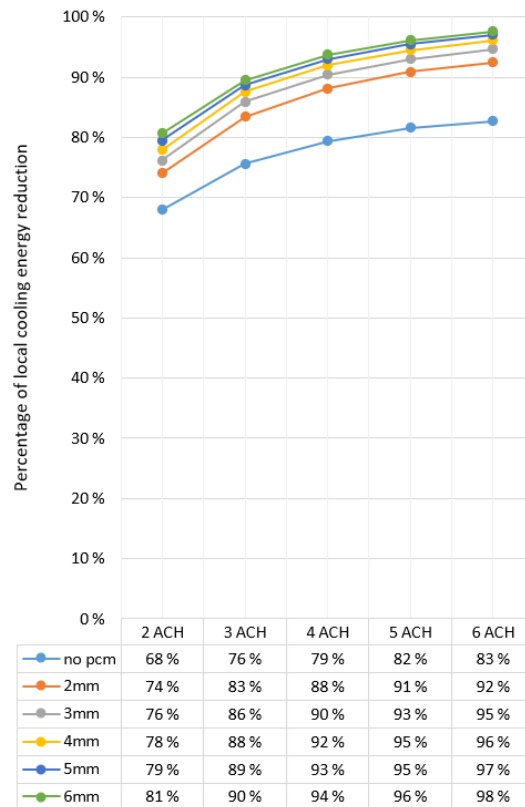


Figure 4.10: Total reduction compared to building with screens

Total energy reduction

Although the local cooling unit is the most affected factor, it is not the only energy post that was affected by the changes. There was also a difference in cooling and auxiliary energy in the AHU, plus the additional energy saved from having the AHU off during NV. Energy posts such as electric heating, lighting, and equipment were not included in the calculations as they were not affected.

The total amount of energy reduction caused by NV and PCM for the two cases are illustrated in figure 4.11, as well as a table showing the percentage of decrease for each simulation. When combining all the energy posts affected by the measures, the decrease in percentage becomes much lower compared to local cooling. This has to do with the small changes in fan usage and cooling done by the AHU, as they were affected to a smaller degree. The results will however give an overview of the total change in energy for every case.

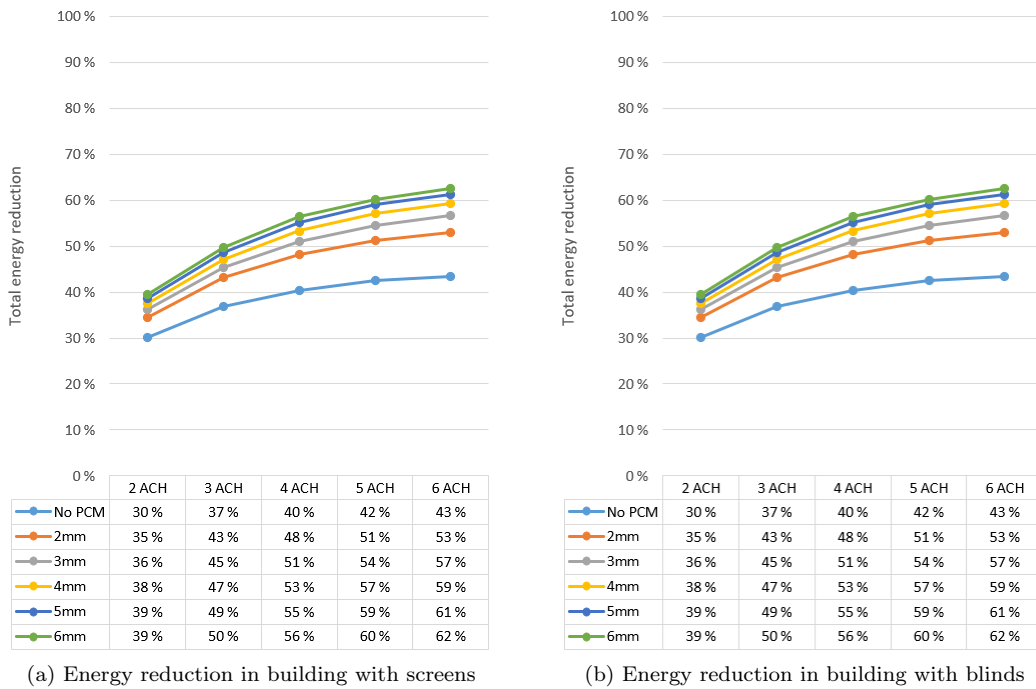


Figure 4.11: Total energy reduction for cooling load and electric use for fans

Although the reduction was not as impacted when combining the energy posts, it is still evident that PCM had a beneficial effect on the total energy. There was also the same visible difference between the two cases. When limiting the heat gain during the day, the need for higher ACH, as well as a thicker layer of PCM becomes less beneficial.

Figure 4.12 shows the maximum reduction to the affected energy posts that were created by implementing all measures (blinds, ACH, PCM), and comparing it to the case with screens that had an energy usage of 2144 kWh. In almost all cases, energy use was reduced by over 50%, with the extreme case of 69% at the highest setting of NV and PCM. All these results give an interesting look at how far it is possible to reduce the cooling load by just implementing a few passive cooling techniques.

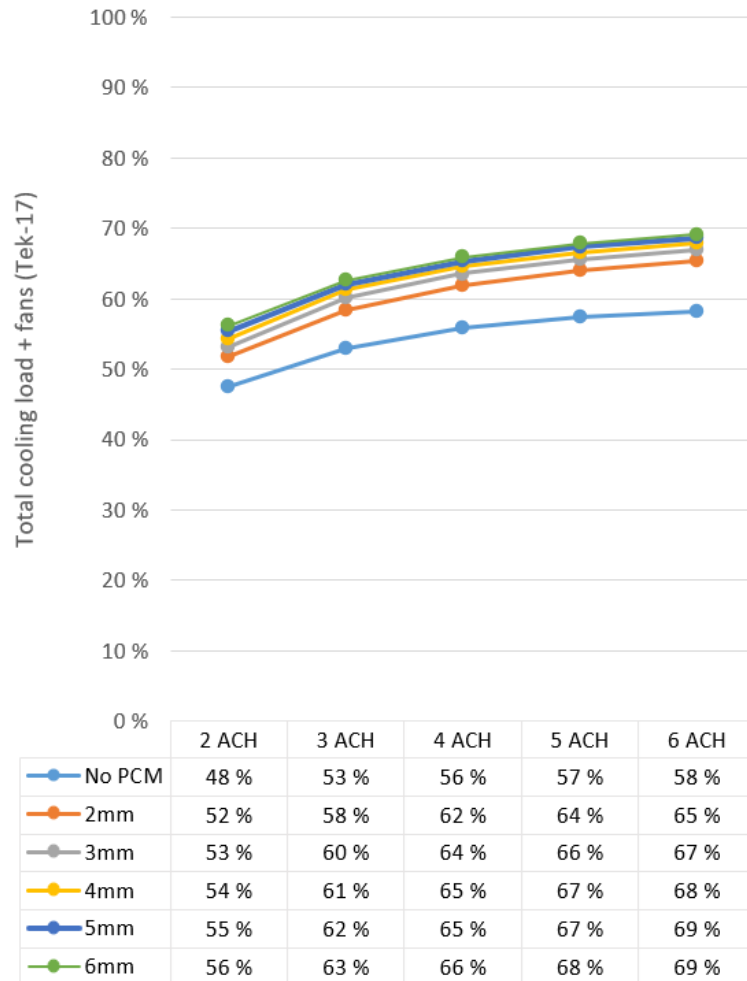


Figure 4.12: Total achieved reduction in reference to building with screens

To get a better understanding of the impact created by the application of PCM, total cooling load was compared to the reference buildings with NV already implemented. Table 4.4 shows the amount of kWh of each case together with the respective reduction in percentage. The differences created by PCM alone varied from case to case and were heavily influenced by the amount of NV. For lower settings such as 2 ACH, applying more PCM from 2mm to 6mm only gave a reduction from 6% to 13%, which may not be profitable in a real-life scenario. There were also clearly diminishing returns when the PCM went above 3mm. As the amount of airflow increased, the effect caused by PCM became more significant. When raising the NV to the highest setting, the reduction created by 2mm PCM almost tripled. A point that can be made here is that if one were to apply the novel PCM spackle to the building, the opportunity to use high amounts of NV is highly beneficial. Not just by getting a lower cooling load caused by NV, but also by amplifying the effect of PCM.

Table 4.4: Energy load reduction compared to reference building

2 ACH			3 ACH			4 ACH		
No PCM	1499 kWh	Reference	No PCM	1353 kWh	Reference	No PCM	1279 kWh	Reference
2mm	1403 kWh	6 %	2mm	1217 kWh	10 %	2mm	1110 kWh	13 %
3mm	1367 kWh	9 %	3mm	1170 kWh	14 %	3mm	1049 kWh	18 %
4mm	1339 kWh	11 %	4mm	1134 kWh	16 %	4mm	1002 kWh	22 %
5mm	1317 kWh	12 %	5mm	1103 kWh	18 %	5mm	963 kWh	25 %
6mm	1299 kWh	13 %	6mm	1077 kWh	20 %	6mm	935 kWh	27 %

5 ACH			6 ACH		
No PCM	1234 kWh	Reference	No PCM	1212 kWh	Reference
2mm	1047 kWh	15 %	2mm	1007 kWh	17 %
3mm	977 kWh	21 %	3mm	931 kWh	23 %
4mm	921 kWh	25 %	4mm	873 kWh	28 %
5mm	880 kWh	29 %	5mm	831 kWh	31 %
6mm	853 kWh	31 %	6mm	805 kWh	34 %

The same comparison was performed in table 4.5 for the case with exterior blinds, to see if there were any differences when the heat gained through the day was more restricted. In these cases, PCM showed a higher percentage of reduction at lower NV settings, but were less effective at 4 ACH and above. The reason it was less effective at higher ACH stems from the amount of energy needed to be removed at night. When limiting solar gain, diminishing returns happened at an increased rate since the maximum amount of energy the PCM could release were achieved at a higher rate.

Table 4.5: Energy load reduction compared to reference building with blinds

2 ACH			3 ACH			4 ACH		
No PCM	1125 kWh	Reference	No PCM	1007 kWh	Reference	No PCM	947 kWh	Reference
2mm	1036 kWh	8 %	2mm	891 kWh	12 %	2mm	817 kWh	14 %
3mm	1005 kWh	11 %	3mm	855 kWh	15 %	3mm	782 kWh	17 %
4mm	979 kWh	13 %	4mm	831 kWh	18 %	4mm	759 kWh	20 %
5mm	957 kWh	15 %	5mm	815 kWh	19 %	5mm	743 kWh	22 %
6mm	939 kWh	17 %	6mm	802 kWh	20 %	6mm	732 kWh	23 %

5 ACH			6 ACH		
No PCM	913 kWh	Reference	No PCM	895 kWh	Reference
2mm	772 kWh	15 %	2mm	744 kWh	17 %
3mm	739 kWh	19 %	3mm	710 kWh	21 %
4mm	716 kWh	22 %	4mm	687 kWh	23 %
5mm	701 kWh	23 %	5mm	673 kWh	25 %
6mm	690 kWh	24 %	6mm	662 kWh	26 %

The correlation between PCM thickness and NV can also be shown by taking the lowest and highest value of NV and focus on the amount of reduction at each PCM thickness. Table 4.6 shows both cases where this was done. For the building using exterior screens, every increase in millimeters gave an additional effect to the cooling load. But after the building was fitted with exterior blinds, this additional effect stopped at around $3mm$. The amount of kWh reduced actually started to decrease.

Table 4.6: Impact of increasing NV at different PCM thickness

(a) Building with screens				
	2 ACH	6 ACH	Difference [kWh]	Reduction [%]
No PCM	1499	1212	287	19 %
2mm	1403	1007	396	28 %
3mm	1367	931	437	32 %
4mm	1339	873	467	35 %
5mm	1317	831	486	37 %
6mm	1299	805	494	38 %

(b) Building with blinds				
	2 ACH	6 ACH	Reduction [kWh]	Reduction [%]
No PCM	1125	895	230	20 %
2mm	1036	744	292	28 %
3mm	1005	710	295	29 %
4mm	979	687	292	30 %
5mm	957	673	285	30 %
6mm	939	662	277	29 %

4.2.3 Solidification of PCM

The temperature on the inside of the PCM layer was logged for every wall and ceiling in the cubicle. An average value was then calculated. The solidification was determined to happen at 20°C. The cases that were analyzed were 2, 4, 6mm of PCM, and 2,4,6 ACH. This was done for the cases with external screens, as well as with exterior blinds. The temperature variation over the course of a week can be seen in 4.13.

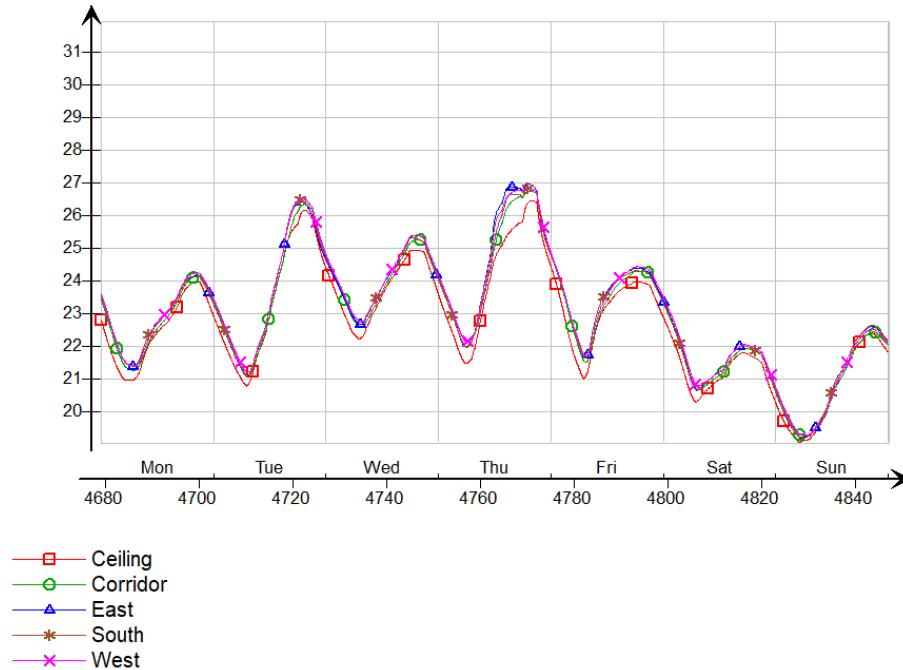


Figure 4.13: Example of PCM temperatures based on location applied

Figure 4.14 shows the number of hours each case reached solidification, compared to the total amount of hours in the month. NV cooling was active 10 hours every day of the month, amounting to 310 hours or 42% of the time. A good indication of an excessive solidification rate would be if the number of hours the PCM spent solidified came close to, or as high as 42%.

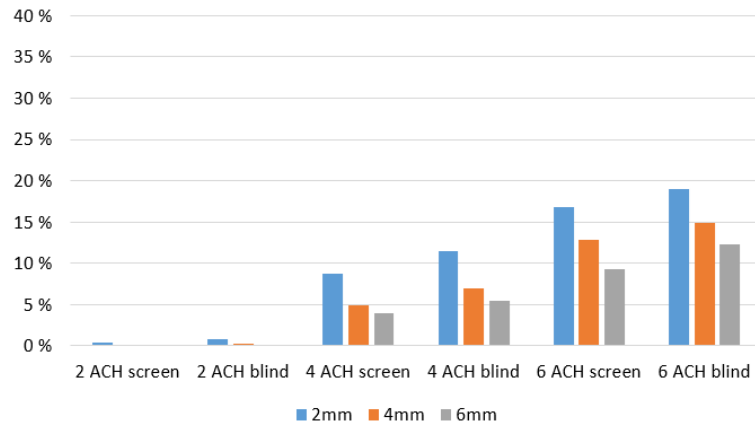


Figure 4.14: Time spend solidified

The results showed that PCM spent almost no hours solidified during the lowest settings of 2 ACH. But started to gradually increase as higher ambient airflow increased. As the simulation month had quite high ambient temperature both during the day and at night, the maximum solidification rate only reached up to 19% or during 141 hours. One interesting finding was that the PCM had an overall higher rate of solidification during the simulations using external blinds. This can be directly connected to the decrease in solar gain, reducing the amount of thermal energy gained during the day and thus making it easier to cool down during the night. The extra time it reached a solid state could be a reason why the effectiveness of PCM was higher in the cases with blinds, and also why diminish rates happened at an increased rate. It was interesting to see that even though solidification was never reached during the cases at low ACH, PCM still played a role in reducing the cooling load.

4.2.4 Fire performance

Euroclass is a classification system that evaluates and categorizes materials based on their fire performance. For this section of the paper, the results sent to the author containing data from its "Cone calorimeter test" was planned to be presented. The data would then be used as input data for the Conetools simulation program, and a representative Euroclass could be found. A desirable outcome would have been a Euroclass of B or higher. In accordance with TEK-17, Euroclass B is the minimum a material can have when applied to interior surfaces and ceilings [40]. Pictures taken from the cone calorimeter test are shown in 4.15

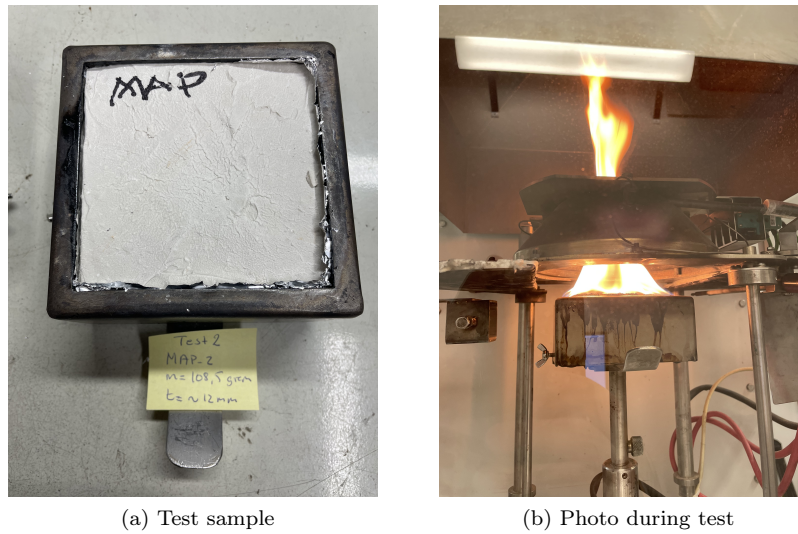


Figure 4.15: Pictures from cone calorimeter test

When examining the test results, some observations suggested that the classification might fall short of the target classification. This was also backed by input from Lund university. Due to these reasons, coupled with time-limitations, no fire performance simulations were performed. A further retrospection should be done towards the chemical composition of the spackling material to achieve the target

4.2.5 Uncertainties and sensitivity analysis

A sensitivity analysis is often important to conduct when the results are not entirely clear, or to check the impact of the inaccuracies that can occur. As all measuring devices often have some form of error, there is always something to be gained from performing an analysis of the result. During the experiment, there were also a couple of problems that arose. Because of the small size of the testing material, it became impossible to place sensors far enough away from the edges of the material. It is therefore a possibility that air leakage could have influenced both the thermocouples and heat flux sensors on both sides. The lack of uniformity in the material also posed a problem during the tests, as it posed a risk of having air gaps under the flux sensors. These problems were dealt with to the best of the authors' ability.

The above mention factors still create uncertainty regarding the calculated thermal conductivity of the PCM spackle. A simple analysis was therefore performed to explore how much this value impacts the end results. Eight additional numerical simulations were run, this time with the heat conductivity value gradually increasing from 0.07 to 0.11. [$W/m \times K$]. Figure 4.7 demonstrates that there are some differences in the outcomes, although they are minor. The case that was used for the changes was one with 4 ACH and a PCM layer thickness of 4mm

Table 4.7: Impact of heat conductivity on electric cooling

Heat conductivity	Electric cooling
0.07	763 kWh
0.0757	762 kWh
0.0814	761 kWh
0.0871	760 kWh
0.0929	760 kWh
0.0986	759 kWh
0.1043	759 kWh
0.11	758 kWh

The total changes created by thermal conductivity only amounted to approximately 5kWh when looking at the extreme points. This indicates that the uncertainties present in the practical experiment did not play a huge factor in the final results of the thesis.

When conducting similar research in the future, the optimal material size itself should have a larger surface area, and be as uniform as possible. Since the specimen that was sent were quite fragile, it's highly likely that extra cracks on the materials surface formed under transport. It could therefore be advantageous to solidify the PCM spackle closer to the test site, to make sure that a minimum amount of cracks is formed.

5. Conclusion

The purpose of this project was to investigate and evaluate a novel phase change material, in the form of a spackle containing microencapsulated paraffin-based PCM. A performance review was also conducted in a "dbf" climate situated in Oslo, Norway. Both experimental tests and numerical simulations were performed. To evaluate the properties of the material, real-life experiments were performed. By using two climate chambers to emulate inside and outside conditions, the amount of heat flux through the material was measured. Using the measured heat flux, surface temperatures, and thickness, the thermal conductivity is found to be $0.093 [W/m \times K]$. This amounted to an increase of $0.013 [W/m \times K]$ when compared to earlier research on a similar material. This result was also quite close to Gyproc's estimated value of 0.1.

Numerical energy simulations were then performed on a validated TEK-17 building in the region of Blindern, Norway. All simulations were performed on the hottest month of the year, which in this case was July. The obtained information of the characteristics of the material was inserted in a PCM module in the numerical simulation software IDA-ICE. Validation of the PCM module has been conducted in a couple of earlier research projects, and showed high accuracy and favorable outcome compared to other similar simulation tools.

The novel PCM spackle was investigated in a portion of the office building, containing only cubicles and one hallway. To get a complete understanding of the novel PCM's influence, 60+ unique simulations were performed. The impact of each parameter change was studied, as well as the impact on the energy efficiency of the building. Overall, the simulations showed various results depending on the building's pre-existing measurements.

Implementing PCM without night ventilation had almost no impact on the energy load of the building. Due to the lack of cooling in the building during the night, the PCM had no time slot where it could release the energy stored during the day.

Simulations on the building had varying PCM thicknesses of 0, 2, 3, 4, 5, 6mm, ACH values of 2,3,4,5,6, as well as two different types of solar shading material. The findings revealed PCM gave a significant reduction in cooling demand, lower peak temperatures, and increased building thermal inertia under the right conditions. Another interesting finding was the difference in cooling load present after the peak temperature of 26°C had been reached. Showing that not only did PCM lower the energy demand by effectively delaying the temperature peak, but also reduced the load by continuing to absorb thermal energy after the peak was reached.

The first 30 simulations only introduced NV and PCM to the reference building. At the lowest NV setting of 2 ACH, only applying 2mm of the spackle gave a 7% decrease, on top of the already 42% reduction from NV alone. However, as the rate of ambient air increased, the role of PCM started to amplify. At the highest value of 6 ACH, the savings gained from applying 2mm went up to 14%. The same development also occurred with higher layer thickness. For the case of 4mm, the reduction went from 12% at 2 ACH, up to 23% at 6 ACH. As the thermal inertia and thermal energy stored in the building body increased, the benefits of more effective cooling were present.

After fitting the building with venetian blinds with a constant slat angle of 45° , another 30 simulations were performed. The reduction created by just changing shading material reduced

the cooling load by 30%, indicating that solar gain played a big role in the thermal increase. The difference created by PCM and NV became enhanced when compared to cases using external screens. At 2 ACH, night ventilation alone went from a reduction of 42% to 54%. And when the same layer of 2mm PCM the additional saving went from 7% to 9%, increasing its effectiveness. Looking at the solidification rates of each simulation, the case with blinds had a higher percentage of hours that reached a solid-state. As the amount of thermal heat gained through the day was lower, PCM had a higher chance of reaching a solid-state during the night. Which resulted in an increase in the PCM's efficiency.

The conclusion that can be drawn is that PCM and NV worked as intended, reducing the overall cooling load by a significant amount. PCM also affected the diurnal thermal fluctuations, as well as kept the cubicles at a desired thermal comfort level for a longer period. The benefits from better solar shading were also evident, making both NV and PCM reduce the cooling load at a higher rate. Adding more PCM showed to be more beneficial when the thermal gain in the cubicle was higher but became an unnecessary measure when the building had reduced solar gain. When introducing PCM, better control over heat gains in the zones can be seen as an important variable. If the building already had some cooling load reduction measures set in place, the attractiveness of implementing PCM grew.

Additional research regarding fire resistance in phase change materials is needed, as the current properties are not suited for practical use in a building. Further improvement in terms of fire resistance is required to fulfill necessary fire codes and standards.

5.1 Future work

Earlier window openings

In further research, it could be interesting to investigate the impact of opening the window earlier in the day. Since the workday ended at 18:00, the local cooling units shut off at that point. A common occurrence that presented itself was the fact that the cubicle still had a temperature rise after this point, which resulted in a higher temperature when NV began. An example of this is shown in figure 5.1. It would be interesting to find out the degree of impact caused by having the windows open at an earlier time.

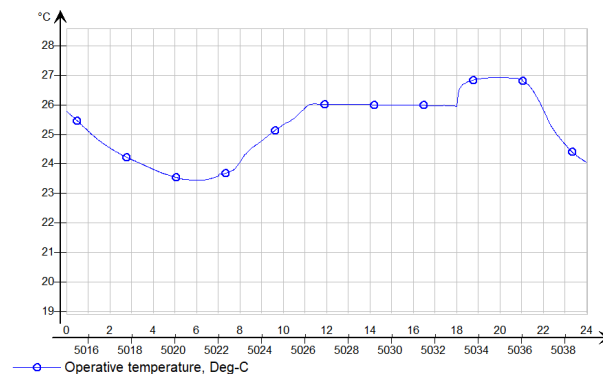


Figure 5.1: Example of temperature rise after 18:00

Longer cooling hours

For the same reason, it would also be interesting to look at the energy use when the cooling hours are prolonged. The idea is that the amount of energy used to cool the building a few extra hours will be gained back the subsequent day with the use of PCM. While writing this thesis, one case was chosen to test out this hypothesis. The building that was chosen was the building with the overall highest PCM temperatures during the month, having external screens with 2 ACH NV and 6mm PCM. The results showed a slight increase in electric cooling, indicating that this would possibly not be a beneficial measure. Further investigation is however needed.

Full shading during unoccupied hours.

Solar shading was set to be drawn when the amount of solar flux reached $100W/m^2$ for all simulations. As a test, one extra case was performed where the additional setting of fully drawing solar shading in the unoccupied hours. This means fully drawn from 18:00-21:00 in the weekdays, and from 07:00-21:00 on weekends. The result showed a small decrease in electric cooling, indicating that this could possibly be used to further reduce the cooling load and also increase the rate of solidification. Because of time restrictions, this could not be performed in this project but would be an interesting variable to investigate in future research.

Bibliography

- [1] “United nations environment programme (2021). 2021 global status report for buildings and construction: Towards a zero-emission, efficient and resilient buildings and construction sector. nairobi,” United Nations Environment Programme, Tech. Rep., 2021. [Online]. Available: <https://www.unep.org/resources/report/2021-global-status-report-buildings-and-construction>
- [2] “The future of cooling,” International Energy Agency, Tech. Rep., 2018. [Online]. Available: <https://www.iea.org/reports/the-future-of-cooling>
- [3] P. Agreement, “Paris agreement,” in *Report of the Conference of the Parties to the United Nations Framework Convention on Climate Change (21st Session, 2015: Paris)*. Retrived December, vol. 4. HeinOnline, 2015, p. 2017.
- [4] G. Deal, “Communication from the commission to the european parliament, the european council, the council, the european economic and social committee and the committee of the regions,” 2018.
- [5] U. Von der Leyen, “A union that strives for more,” *My agenda for Europe. Political guidelines for the next European Commission*, vol. 2024, p. 2019, 2019.
- [6] B. Aebischer, G. Catenazzi, and M. Jakob, “Impact of climate change on thermal comfort, heating and cooling energy demand in europe,” in *Proceedings eceee*, 2007, pp. 859–870.
- [7] M. A. Kamal, “An overview of passive cooling techniques in buildings: design concepts and architectural interventions,” *Acta Technica Napocensis: Civil Engineering & Architecture*, vol. 55, no. 1, pp. 84–97, 2012.
- [8] N. Artmann, H. Manz, and P. Heiselberg, “Climatic potential for passive cooling of buildings by night-time ventilation in europe,” *Applied energy*, vol. 84, no. 2, pp. 187–201, 2007.
- [9] K. Pielichowska and K. Pielichowski, “Phase change materials for thermal energy storage,” *Progress in materials science*, vol. 65, pp. 67–123, 2014.
- [10] M. F. Demirbas, “Thermal energy storage and phase change materials: an overview,” *Energy Sources, Part B: Economics, Planning, and Policy*, vol. 1, no. 1, pp. 85–95, 2006.
- [11] F. Kuznik, D. David, K. Johannes, and J.-J. Roux, “A review on phase change materials integrated in building walls,” *Renewable and Sustainable Energy Reviews*, vol. 15, no. 1, pp. 379–391, 2011. [Online]. Available: <https://www.sciencedirect.com/science/article/pii/S1364032110002716>

- [12] A. Abhat, "Low temperature latent heat thermal energy storage: heat storage materials," *Solar energy*, vol. 30, no. 4, pp. 313–332, 1983.
- [13] P. Sittisart and M. M. Farid, "Fire retardants for phase change materials," *Applied Energy*, vol. 88, no. 9, pp. 3140–3145, 2011.
- [14] Y. Cai, Y. Hu, L. Song, Y. Tang, R. Yang, Y. Zhang, Z. Chen, and W. Fan, "Flammability and thermal properties of high density polyethylene/paraffin hybrid as a form-stable phase change material," *Journal of Applied Polymer Science*, vol. 99, no. 4, pp. 1320–1327, 2006.
- [15] A. Sharma, V. V. Tyagi, C. R. Chen, and D. Buddhi, "Review on thermal energy storage with phase change materials and applications," *Renewable and Sustainable energy reviews*, vol. 13, no. 2, pp. 318–345, 2009.
- [16] S. Hasnain, "Review on sustainable thermal energy storage technologies, part i: heat storage materials and techniques," *Energy conversion and management*, vol. 39, no. 11, pp. 1127–1138, 1998.
- [17] A. S. Fleischer, *Thermal energy storage using phase change materials: fundamentals and applications*. Springer, 2015.
- [18] M. B. Hoy, "Smart buildings: an introduction to the library of the future," *Medical reference services quarterly*, vol. 35, no. 3, pp. 326–331, 2016.
- [19] S. Jørgensen, "Sintef technical approval, tg 2135," SINTEF, Tech. Rep., 2021. [Online]. Available: <https://www.sintefcertification.no/product/index/129>
- [20] "Reaction to fire tests for building products — building products excluding floorings exposed to the thermal attack by a single burning item," Standard Norge, Standard, 2020.
- [21] Hukseflux, *Hukseflux Thermal Sensors, User manual HFP01/HFP03, manual version 1721*, 2022.
- [22] C. H. Spink, "Differential scanning calorimetry," *Methods in cell biology*, vol. 84, pp. 115–141, 2008.
- [23] "Reaction-to-fire tests — heat release, smoke production and mass loss rate — part 1: Heat release rate (cone calorimeter method) and smoke production rate (dynamic measurement)," International Standardization Organization, Standard, 2015.
- [24] V. Babrauskas and R. Peacock, "Heat release rate: The single most important variable in fire hazard," *Fire Safety Journal*, vol. 18, pp. 255–272, 12 1992.
- [25] J. Lindholm, A. Brink, and M. Hupa, "Cone calorimeter - a tool for measuring heat release rate," 01 2009.
- [26] "Reaction to fire tests for building products — building products excluding floorings exposed to the thermal attack by a single burning item," Standard Norge, Standard, 2020.
- [27] M. Hjohlman, P. Andersson, and P. Van Hees, "Flame spread modelling of complex textile materials," *Fire technology*, vol. 47, no. 1, pp. 85–106, 2011.
- [28] E. S. AB, "Ida ice." [Online]. Available: <https://www.equa.se/en/ida-ice>

- [29] D. Mazzeo, N. Matera, C. Cornaro, G. Oliveti, P. Romagnoni, and L. De Santoli, “Energyplus, ida ice and trnsys predictive simulation accuracy for building thermal behaviour evaluation by using an experimental campaign in solar test boxes with and without a pcm module,” *Energy and Buildings*, vol. 212, p. 109812, 2020.
- [30] A. Aamodt, A. Chaudhuri, H. B. Madessa, and T. A. Vik, “On the energy performance of micro-encapsulated phase change material enhanced spackling with night ventilation,” *Applied Sciences*, vol. 11, no. 4, p. 1472, 2021.
- [31] SINTEF, “344.110 tilpasningsdyktige kontorbygninger,” Byggforskserien, Tech. Rep., 2004. [Online]. Available: https://www.byggforsk.no/dokument/3223/tilpasningsdyktige_kontorbygninger#i4
- [32] M. Kottek, J. Grieser, C. Beck, B. Rudolf, and F. Rubel, “World map of the köppen-geiger climate classification updated,” 2006.
- [33] “Hygrothermal performance of buildings - calculation and presentation of climatic data - part 4: Hourly data for assessing the annual energy use for heating and cooling (iso 15927-4:2005),” International Standardization Organization, Standard, 2005.
- [34] M. Kolokotroni, B. Webb, and S. Hayes, “Summer cooling with night ventilation for office buildings in moderate climates,” *Energy and Buildings*, vol. 27, no. 3, pp. 231–237, 1998.
- [35] B. Givoni, “Effectiveness of mass and night ventilation in lowering the indoor daytime temperatures. part i: 1993 experimental periods,” *Energy and Buildings*, vol. 28, no. 1, pp. 25–32, 1998.
- [36] V. Geros, M. Santamouris, A. Tsangrasoulis, and G. Guarracino, “Experimental evaluation of night ventilation phenomena,” *Energy and Buildings*, vol. 29, no. 2, pp. 141–154, 1999.
- [37] T. E. Kuhn, C. Bühler, and W. J. Platzer, “Evaluation of overheating protection with sun-shading systems,” *Solar Energy*, vol. 69, pp. 59–74, 2001.
- [38] G. Kim, H. S. Lim, T. S. Lim, L. Schaefer, and J. T. Kim, “Comparative advantage of an exterior shading device in thermal performance for residential buildings,” *Energy and buildings*, vol. 46, pp. 105–111, 2012.
- [39] M. Rabani, H. B. Madessa, and N. Nord, “Achieving zero-energy building performance with thermal and visual comfort enhancement through optimization of fenestration, envelope, shading device, and energy supply system,” *Sustainable Energy Technologies and Assessments*, vol. 44, p. 101020, 2021.
- [40] “Byggteknisk forskrift (tek17), § 11-9. materialer og produkters egenskaper ved brann,” Direktoratet for byggkvalitet, Tech. Rep., 20017. [Online]. Available: <https://dibk.no/regelverk/byggteknisk-forskrift-tek17/11/iii/11-9/>


A. PCM properties

The screenshot shows the 'Pc-Material' window in IDA ICE. The title bar reads 'Pc-Material © PCM_gyproc_5dpm_final'. Below the title bar, the material name 'PCM_gyproc_5dpm_final' is displayed next to a 'Default' dropdown menu. A 'Parameters' section contains a table with the following data:

Name	Value	Unit	Description
N	287	items	Number of temperature coordinates
NM1	286.0	items	Number of partial enthalpies (N-1)
RHOSOL	970.0	kg/m ³	Layer density (solid)
CPSOL	1600.0	J/(kg K)	Layer specific heat (solid) (J/(kg K))
LAMBDA SOL	0.093	W/(m K)	Layer heat conductivity (solid) (W/(m K))
CPLIQ	1810.0	J/(kg K)	Layer specific heat (liquid) (J/(kg K))
LAMBDA LIQ	0.093	W/(m K)	Layer heat conductivity (liquid) (W/(m K))
C0	14300.0	J/(kg K)	Specific heat during reversing (c0 ≤ min(cpSol...)
TH[1:287]	{12.047 12.1295...}	°C	Temperatures at which melting/solidifying enthal...
DHDTMELT[1:286]	{3467.208 3501....}	J/(kg K)	Partial enthalpies between temperature coordin...
DHDT SOLID[1:286]	{3467.208 3501....}	J/(kg K)	Partial enthalpies between temperature coordin...

Figure A.1: PCM properties inserted in IDA ICE

B. Input data report

		Input data Report	
Project		Building	
		Model floor area	636.0 m ²
Customer		Model volume	1084.4 m ³
Created by	Sebastian	Model ground area	0.0 m ²
Location	Blindern-Oslo	Model envelope area	558.7 m ²
Climate file	Blindern 2003-2013	Window/Envelope	12.6 %
Case	TEK-17 reference case	Average U-value	0.3886 W/(m ² K)
Simulated	13.05.2022 09:07:38	Envelope area per Volume	0.5153 m ² /m ³

Wind driven infiltration airflow rate 451.418 l/s at 50.000 Pa

Building envelope	Area [m ²]	U [W/(m ² K)]	U*A [W/K]	% of total
Walls above ground	170.62	0.22	37.54	17.29
Rendered l/w concrete wall 250	53.91	0.22	11.86	5.46
Rendered l/w concrete wall 250 PCM	116.71	0.22	25.68	11.83
Walls below ground	0.00	0.00	0.00	0.00
Roof	318.00	0.18	57.24	26.36
Concrete joist roof	318.00	0.18	57.24	26.36
Floor towards ground	0.00	0.00	0.00	0.00
Floor towards amb. air	0.00	0.00	0.00	0.00
Windows	70.13	1.20	84.17	38.77
Triple with suspended low-e film (argon) (WIN7)	70.13	1.20	84.17	38.77
Doors	0.00	0.00	0.00	0.00
Thermal bridges			38.16	17.58
Total	558.75	0.39	217.12	100.00

Thermal bridges	Area or Length	Avg. Heat conductivity	Total [W/K]
External wall / internal slab	211.80 m	0.000 W/(m K)	0.000
External wall / internal wall	131.02 m	0.000 W/(m K)	0.000
External wall / external wall	6.82 m	0.000 W/(m K)	0.000
External windows perimeter	178.72 m	0.000 W/(m K)	0.000
External doors perimeter	0.00 m	0.000 W/(K m)	0.000
Roof / external walls	70.60 m	0.000 W/(m K)	0.000
External slab / external walls	0.00 m	0.000 W/(K m)	0.000
Balcony floor / external walls	0.00 m	0.000 W/(K m)	0.000
External slab / Internal walls	0.00 m	0.000 W/(K m)	0.000
Roof / Internal walls	60.00 m	0.000 W/(m K)	0.000
External walls, inner corner	0.00 m	0.000 W/(K m)	0.000
Roof / external walls, inner corner	0.00 m	0.000 W/(K m)	0.000
External slab / external walls, inner corner	0.00 m	0.000 W/(K m)	0.000
Total envelope (incl. roof and ground)	558.75 m²	0.068 W/(m² K)	38.160
Extra losses	-	-	0.000
Sum	-	-	38.161

Windows	Area [m ²]	U Glass [W/(m ² K)]	U Frame [W/(m ² K)]	U Total [W/(m ² K)]	U*A [W/K]	Shading factor g
E	5.04	1.13	1.86	1.20	6.05	0.53
S	60.05	1.13	1.86	1.20	72.08	0.53
W	5.04	1.13	1.86	1.20	6.05	0.53
Total	70.13	1.13	1.86	1.20	84.17	0.53

Air handling unit	Pressure head supply/exhaust [Pa/Pa]	Fan efficiency supply/exhaust [-/-]	System SFP [kW/(m ³ /s)]	Heat exchanger temp. ratio/min exhaust temp. [-/°C]
AHU	900.00/600.00	0.60/0.60	1.50/1.00	0.90/1.00
hallway1	600.00/400.00	0.60/0.60	1.00/0.67	0.60/1.00

Figure B.1: Input data report

C. Shading properties

The screenshot shows a software window titled "Shade material" with a dropdown menu set to "Diffusing shade material (WIN7)". The window contains several input fields for material properties:

Shade material	Transmittance	Outside (upper for slats) Reflectance	Inside (lower for slats) Reflectance
Total shortwave	0.5	0.3	0.3
Visible	0.4	0.2	0.2
Diffusion	1.0	1.0	1.0
Longwave	0.0	Emissivity	
		0.84	0.84
Thickness	0.6 mm		
k	0.9 W/(K.m)		
Ventilation			
Openess factor	0.0 m ² /m ²		

Figure C.1: Screen shade properties

The screenshot shows a software window titled "Exterior screen" with a dropdown menu set to "Generic screen shade". It includes a diagram of a screen on a window and a stick figure for scale. The diagram shows a screen with a height of 0.07 m. Below the diagram, there are input fields for "Temperature limit" (°C) and "Wind limit" (m/s). A "Ventilation" section contains a diagram of a screen with gaps: "Top gap" (0.01 m), "Side gap" (0.01 m), and "Bottom gap" (0.01 m). A "Description" text area is also present.

Figure C.2: Caption

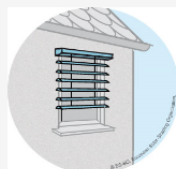
Shade material

Shade material	Transmittance	Outside (upper for slats) Reflectance	Inside (lower for slats) Reflectance
Total shortwave	<input type="text" value="0.0"/>	<input type="text" value="0.35"/>	<input type="text" value="0.35"/>
Visible	<input type="text" value="0.0"/>	<input type="text" value="0.35"/>	<input type="text" value="0.35"/>
Diffusion	<input type="text" value="1.0"/>	<input type="text" value="1.0"/>	<input type="text" value="1.0"/>
Longwave	<input type="text" value="0.0"/>	Emissivity	
		<input type="text" value="0.9"/>	<input type="text" value="0.9"/>
Thickness	<input type="text" value="1"/> mm		
k	<input type="text" value="100"/> W/(K.m)		
Ventilation			
Openess factor	<input type="text" value="0.0"/> m ² /m ²		

Figure C.3: Blind shade properties

Exterior venetian blind

Exterior venetian blind



Exterior venetian blind

[Slat material](#)

Spacing mm

Slat width mm

Temperature limit °C

Wind limit m/s

Description

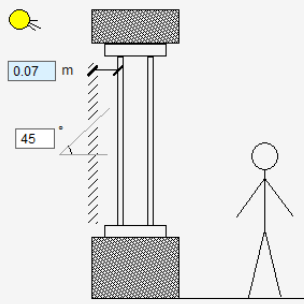


Figure C.4: Blind shade placement

D. Measurements from the Hukseflux TRSYS01 system

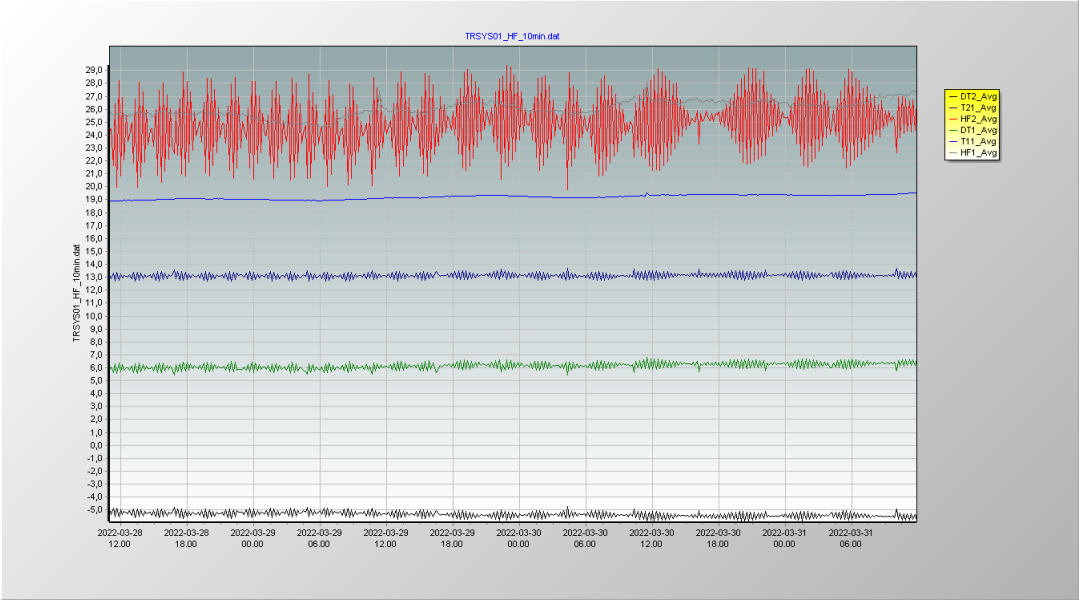


Figure D.1: Results from TRSYS01 over a three day period